Evolution of the Longmen Shan Foreland Basin (Western Sichuan, China) during the Late Triassic Indosinian Orogeny

Article *in* Basin Research · March 2003

DOI: 10.1046/j.1365-2117.2003.00197.x · Source: OAI

4 authors, including:

Yong Li
Chengdu University of Technology
208 PUBLICATIONS **2,915** CITATIONS
SEE PROFILE

Philip A. Allen
Imperial College London
134 PUBLICATIONS **6,049** CITATIONS
SEE PROFILE

Basin Research (2003) **15,** 117–138

Evolution of the Longmen Shan Foreland Basin (Western Sichuan, China) during the Late Triassic Indosinian Orogeny

L. Yong,* P. A. Allen,† A. L. Densmore† and X. Qiang‡

**Institute of Sedimentary Geology, Chengdu University of Technology, Chengdu, 610059, Peoples Republic of China*
†Department of Earth Sciences, ETH Zentrum, Sonneggstrasse 5, CH-8092 Zürich, Switzerland
‡Chengdu Institute of Geology and Mineral Resources, Chengdu, 610082, Peoples Republic of China

ABSTRACT

The Longmen Shan Foreland Basin developed as a flexural foredeep during the Late Triassic Indosinian orogeny, spanning the time period c. 227–206 Ma. The basin fill can be divided into three tectonostratigraphic units overlying a basal megasequence boundary, and is superimposed on the Palaeozoic–Middle Triassic (Anisian) carbonate-dominated margin of the South China Block. The remains of the load system responsible for flexure of the South China foreland can be seen in the Songpan-Ganzi Fold Belt and Longmen Shan Thrust Belt. Early in its history the Longmen Shan Foreland Basin extended well beyond its present northwestern boundary along the trace of the Pengguan Fault, to at least the palinspastically restored position of the Beichuan Fault.

The basal boundary of the foreland basin megasequence is a good candidate for a flexural forebulge unconformity, passing from conformity close to the present trace of the Beichuan Fault to a karstified surface towards the southeast. The overlying tectonostratigraphic unit shows establishment and drowning of a distal margin carbonate ramp and sponge build-up, deepening into offshore marine muds, followed by progradation of marginal marine siliciclastics, collectively reminiscent of the Alpine underfilled trinity of Sinclair (1997). Tectonostratigraphic unit 2 is marked by the severing of the basin's oceanic connection, a major lake flooding and the gradual establishment of major deltaic-paralic systems that prograded from the eroding Longmen Shan orogen. The third tectonostratigraphic unit is typified by coarse, proximal conglomerates, commonly truncating underlying rocks, which fine upwards into lacustrine shales.

The foreland basin stratigraphy has been further investigated using a simple analytical model based on the deflection by supracrustal loads of a continuous elastic plate overlying a fluid substratum. Load configurations have been partly informed by field geology and constrained by maximum elevations and topographic profiles of present-day mountain belts. The closest match between model predictions and stratigraphic observations is for a relatively rigid plate with flexural rigidity on the order of 5×10^{23} to 5×10^{24} N m (equivalent elastic thickness of c. 43–54 km). The orogenic load system initially (c. 227–220 Ma) advanced rapidly (>15 mm yr^{-1}) towards the South China Block in the Carnian, associated with the rapid closure of the Songpan-Ganzi ocean, before slowing to < 5 mm yr^{-1} during the sedimentation of the upper two tectonostratigraphic units (c. 220–206 Ma).

INTRODUCTION

Although the generalities of foreland basin evolution and the forcing tectonic mechanisms are now widely recognised (Jordan, 1981; Stockmal *et al.*, 1986; Flemings & Jordan, 1990; Beaumont *et al.*, 1991; Sinclair *et al.*, 1991; DeCelles & Giles, 1996), a number of important questions remain to be answered satisfactorily. Many of these questions concern the precise sensitivity of the stratigraphic record of foreland basins to variations in the flexural rigidity (or elastic thickness) of the continental lithosphere in space and time, the kinematics and configuration of the load system driving flexure, and the spatial pattern, vigour and response times of the surface process systems responsible

Correspondence: Philip A. Allen, Department of Earth Sciences, ETH-Zentrum, Sonneggstrasse 5, CH-8092 Zürich, Switzerland. E-mail: philip.allen@erdw.ethz.ch

for mountain belt denudation and sediment transport to neighbouring depocentres. The sedimentary fills of ancient foreland basins formed in a wide range of different geodynamic (and climatic) settings therefore provide a valuable window into some of the fundamental relationships between mountain building and basin development.

The eastern margin of the Tibetan Plateau in central Asia is formed by the > 500 km long ranges of the Longmen Shan (Fig. 1). The peaks of the Longmen Shan rise abruptly from the western Sichuan Basin to altitudes of over 5000 m. The present day Longmen Shan mountain front coincides approximately with the position of a Mesozoic collisional plate margin that developed as the Palaeo-Tethys ocean was closed and the North Tibetan (Qiangtang) Block sutured to the colliding North China–Kunlun–Qaidam and South China Blocks (Sengör, 1985; Yin & Nie, 1996; Zhou & Graham, 1996).

The Longmen Shan Thrust Belt represents part of the orogenic load system that deflected down the lithosphere of the South China Block to form the foreland basin situated to the southeast in Sichuan Province (Chen *et al*., 1994, 1995; Burchfiel *et al*., 1995; Chen & Wilson, 1996; Korsch *et al*., 1997). The deformation in the Longmen Shan Thrust Belt was initiated in the Indosinian Orogeny (Late Triassic), and continued through to the Early Cretaceous (Yenshanian Orogeny), with a reactivation in the Late Miocene due to the India–Asia collision (Wang *et al*., 1989). The adjacent sedimentary basin in western Sichuan contains a westward thickening, several-kilometres thick succession of Upper Triassic sedimentary rocks that were deposited coeval with deformation in the Longmen Shan. These strata overlie the older, thick (> 5 km), carbonate-dominated stratigraphy (Devonian–Middle Triassic) of the South China Block. We make a distinction in this

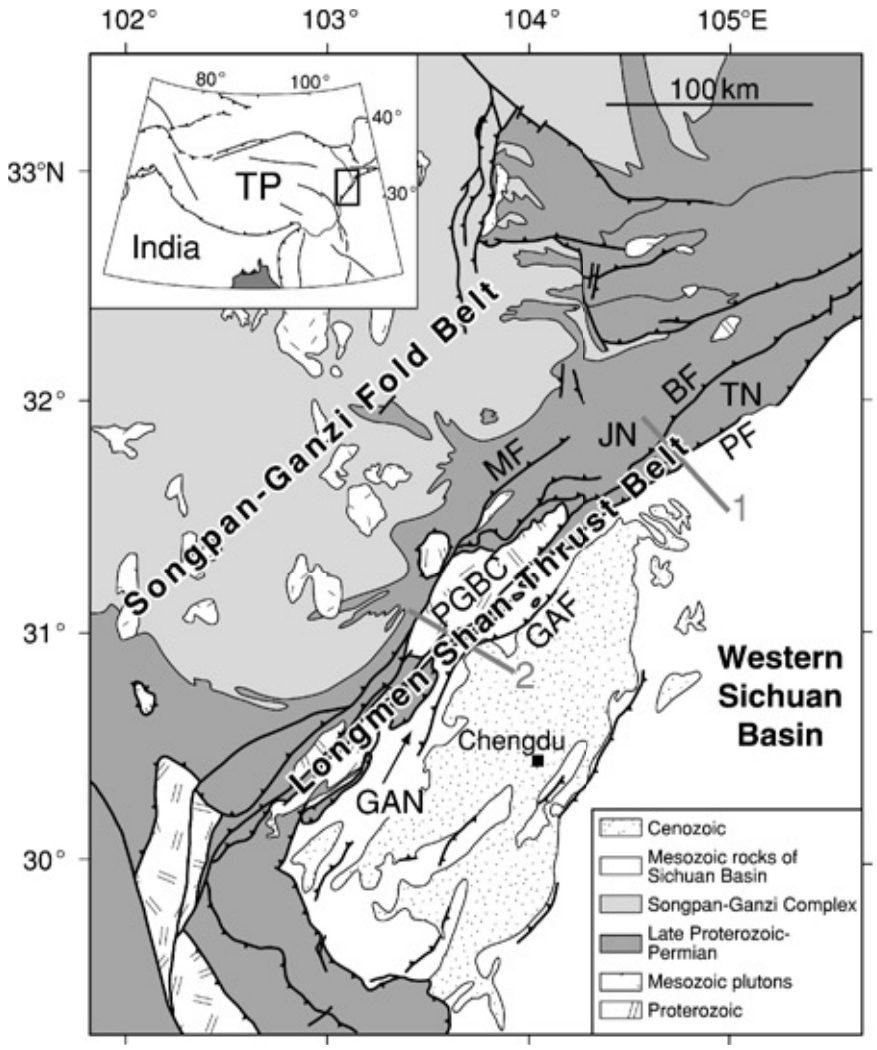

Fig. 1. General geology and tectonic setting of the Longmen Shan region, modified from Kirby *et al.* (2000) and Burchfiel *et al.* (1995). Inset shows the Longmen Shan region with respect to the Tibetan Plateau and the Cenozoic India–Asia collision. TP, Tibetan Plateau. Main map shows the principal tectonic units in the Songpan-Ganzi Fold Belt and Longmen Shan Thrust Belt. Barbs show thrust faults. Grey lines show locations of cross-sections in Fig. 2. Nappes and tectonic units: GAN, Guanxian-Anxian Nappe; JN, Jiuding Shan Nappe; PGBC, Pengxian-Guanxian Basement Complex; TN, Tangwangzhai Nappe. Faults: MF, Maowen Fault; BF, Beichuan Fault; PF, Pengguan Fault; GAF, Guanxian-Anxian Fault.

paper between the Sichuan Basin, which is a present-day lowland region containing depocentres that record sedimentation between Late Triassic and Quaternary, and the Longmen Shan Foreland Basin, which contains an Upper Triassic megasequence related to Indosinian deformational events in the adjacent Longmen Shan thrust belt.

Our aim in this paper is to describe the large-scale sedimentary architecture of the basin fill and, using a simple one-dimensional forward model, to demonstrate that the Longmen Shan Foreland Basin can be explained in outline by flexure of the South China lithosphere in response to Indosinian loading. Using the analytical model, the spatial extent, thickness and gross depositional environments of foreland basin tectonostratigraphic units allow a plausible combination of elastic thickness of the South China lithosphere, load configuration and load advance rate to be estimated.

GEOLOGICAL HISTORY

From northwest to southeast, the eastern margin of the Tibetan Plateau is composed of three major tectonic units: the Songpan-Ganzi Fold Belt, the Longmen Shan Thrust Belt, and the Longmen Shan Foreland Basin superimposed on the lithosphere of the South China Block (Figs 1–3).

In summary, the Songpan-Ganzi Fold Belt comprises a metamorphosed and deformed stratigraphic succession of Mesoproterozoic basement (1017–1043 Ma U–Pb ages, Luo & Long, 1992), unconformably overlain by Neoproterozoic (Sinian) volcanic rocks and dolomite. These rocks in turn are overlain by very thick (>10 km) lower Palaeozoic to Upper Triassic sedimentary rocks of the Songpan-Ganzi Complex, which range from pelagic micrites and olistostromal deposits to siliciclastic turbidites (Zhou & Graham, 1996). The Songpan-Ganzi Complex is overlain unconformably by post-Indosinian uppermost Triassic or lowest Jurassic sandstones and felsic volcanic rocks (Huang & Chen, 1987; Liu *et al*., 1992) (Fig. 3). A stratigraphic gap in the Songpan-Ganzi Fold Belt occupies the time interval of coarse clastic sedimentation of the Xujiahe Group in the Longmen Shan Foreland Basin to the southeast. In contrast, the South China Block cover is composed of a thick (> 5 km) succession of unmetamorphosed and relatively undeformed Devonian to Middle Triassic carbonate. In the south the < 3 km-thick Emei Shan basalts erupted during thermal doming and extension in the Late Permian (Luo *et al*., 1990). The broad, regional picture in the Triassic prior to the formation of the Longmen Shan Foreland Basin is therefore of a shallow water to emergent continental margin in the SE passing to the NW into a deep, rapidly subsiding turbiditic trough, commonly interpreted as a remnant ocean basin (Yin & Nie, 1996; Ingersoll *et al*., 1995; Zhou & Graham, 1996). The Longmen Shan Thrust Belt comprises both the telescoped, unmetamorphosed, shallow water carbonate-dominated passive margin of the South China Block and its crystalline basement, and the folded and thrusted deep marine metasediments deposited in Palaeo-Tethys. Since the turbidites of the Songpan-Ganzi Complex range in age up to Late Triassic, and the initial deposits of the Longmen Shan Foreland Basin are Carnian in age (Maantang Formation) (see next section), sedimentation must have continued as the remnant ocean basin was progressively shortened and rapidly incorporated into an Indosinian orogenic wedge.

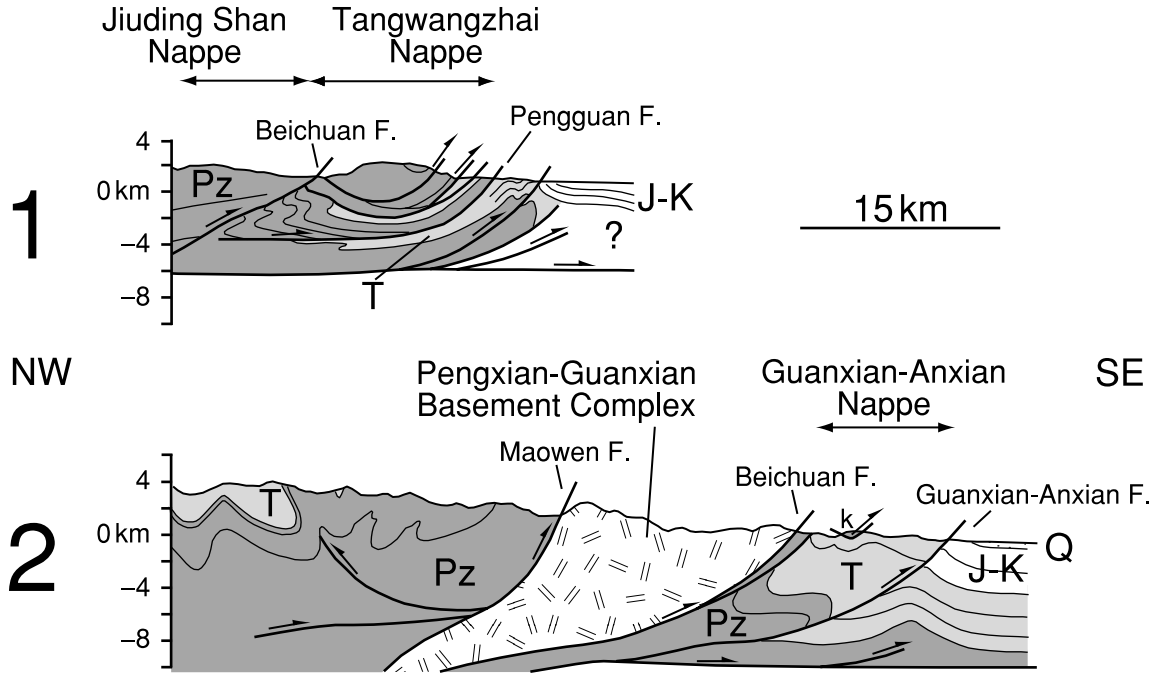

Fig. 2. Structural cross-sections through the eastern Longmen Shan Thrust Belt and western Sichuan Basin, located in Fig. 1. Lithological ornaments as in Fig. 1. Simplified from Burchfiel *et al*. (1995).

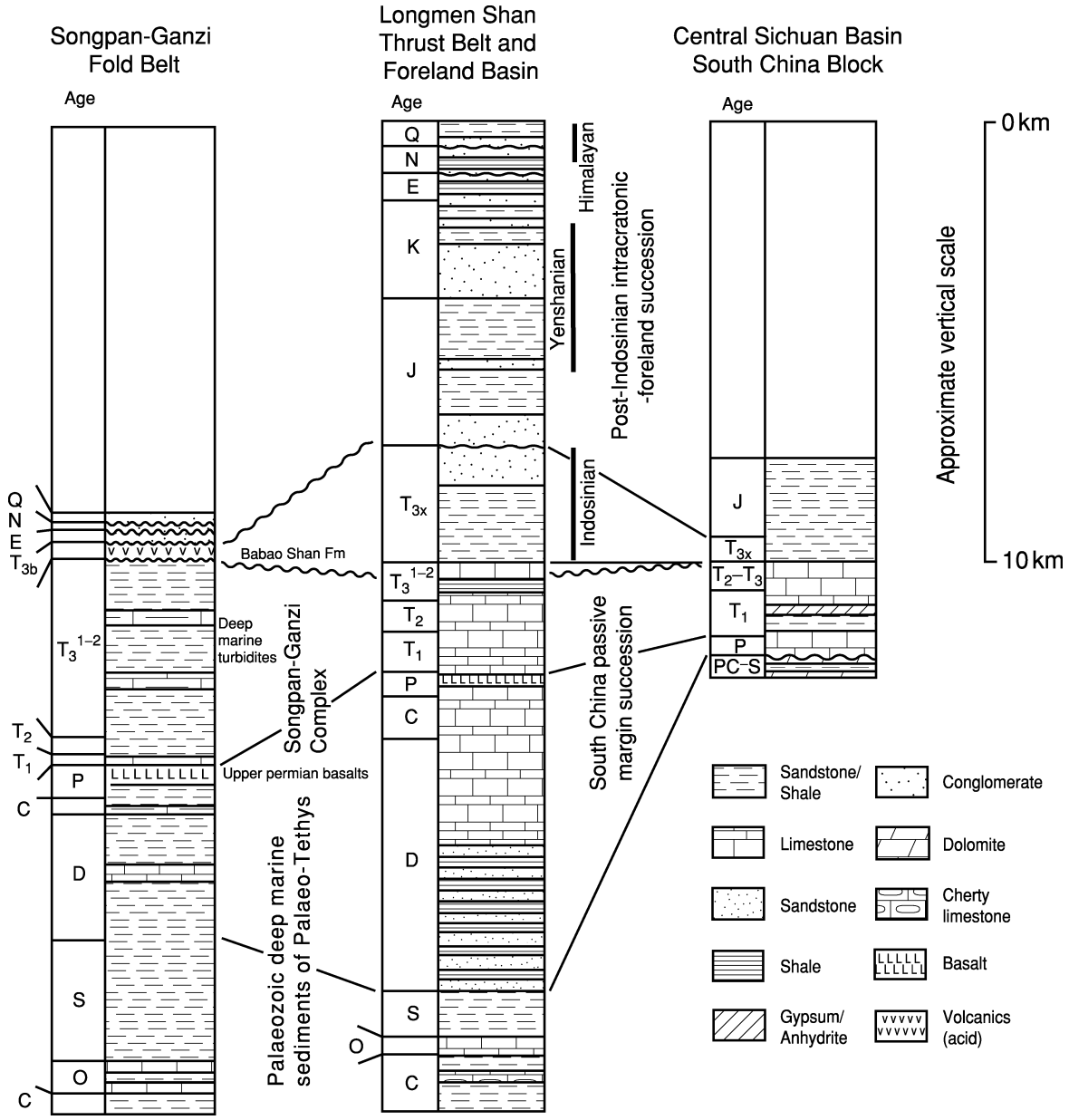

Fig. 3. Generalised stratigraphic columns from Songpan-Ganzi Fold Belt, Longmen Shan Thrust Belt and Foreland Basin, and South China Block in central Sichuan Basin, showing the lateral change from the carbonate-dominated passive margin succession of the South China Block to the deep-water turbidites of the Songpan-Ganzi Complex. The Indosinian foreland basin megasequence is superimposed on the western edge of the South China Block. T_1, T_2 and T_3 refer to Lower, Middle and Upper Triassic, respectively. T_{3x} refers to the Upper Triassic Xujiahe Group. Modified from Chen *et al.* (1995).

The Songpan-Ganzi Fold Belt

The Songpan-Ganzi Fold Belt is the southeastern member of a network of Permo–Triassic mobile belts that stretches from the Pamir, across the ranges of the Kunlun and into southwest China. It is enclosed to the south by the Cimmerian fragments of North Tibet (Qiangtang) and to the north by the Permian margin of Eurasia. The Songpan-Ganzi Fold Belt is dominated by deformed lower-greenschist facies Triassic sedimentary rocks, including both pelagic micrites and siliciclastic turbidites, reaching 6 km in thickness in the central portion of the Fold Belt (Zou *et al.*, 1984; Rao & Xu, 1987). It is only along the southeastern margin of the Fold Belt that upper greenschist to amphibolite facies Triassic turbidites and Palaeozoic greywacke-shales of the western South China margin are exposed. The Palaeozoic–Triassic units were metamorphosed, shortened and deformed during the Indosinian Orogeny (Zhang, 1981; Hu *et al.*, 1983; Deng & Li, 1987; Xu *et al.*, 1992; Burchfiel *et al.*, 1995; Zhou & Graham, 1996) and were locally unconformably overlain by post-orogenic siliciclastics, acidic volcanics and coal of

latest Triassic age (T_{3b} – the Babao Shan Formation; Hong, 1991; Long, 1991) (Fig. 3). This implies that intermontane basins existed at the close of the Triassic.

The Longmen Shan Thrust Belt

The Longmen Shan Thrust Belt, approximately 500 km long and 30–50 km wide, defines a major part of the highly dissected eastern margin of the Tibetan Plateau. The stratigraphic pile in the Longmen Shan is subdivided into tectonic units bounded by four regionally significant, NW-dipping thrust faults – from northwest to southeast, the Maowen, Beichuan, Pengguan, and Guanxian-Anxian Faults (Chen *et al.*, 1995; Chen & Wilson, 1996) (Figs 1 and 2). Note that the Pengguan Fault as used here is equivalent to the Xiangshui Fault of Chen & Wilson (1996). Each tectonic unit, emplaced during the Indosinian orogeny, has its own stratigraphic and deformational features. From northwest to southeast, these units are:

Pengxian-Guanxian Basement Complex comprises Mesoproterozoic granitic basement and Neoproterozoic cover unconformably overlain by Devonian–Triassic carbonate, demonstrating that this crystalline basement cored massif was a topographic high during the Devonian–Triassic relative to the deep and rapidly subsiding basin preserved in the Songpan-Ganzi Fold Belt. The youngest sedimentary rocks involved in thrusting are Lower Triassic carbonate. The basement complex is viewed as a system of basement-involved slices emplaced in the early Indosinian Orogeny (Chen & Wilson, 1996). The nappe is bounded by the Maowen Fault to the north and the Beichuan Fault to the south (Figs 1 and 2).

Jiuding Shan Nappe consists principally of Palaeozoic turbidites metamorphosed to lower greenschist grade, emplaced southeastwards by thrusts incorporating Mesoproterozoic basement slices (Chen & Wilson, 1996). The nappe forms the hanging wall of the Beichuan Fault in the northern Longmen Shan. The main difference with the Pengxian-Guanxian Basement Complex is therefore that the Jiuding Shan Nappe contains a metamorphosed deep-water stratigraphy (Chen *et al.*, 1995).

Tangwangzhai Nappe comprises a Devonian to Upper Triassic unmetamorphosed carbonate-rich succession deformed into large open folds, emplaced over Upper Triassic Xujiahe Group (T_{3x}) of the Indosinian foreland basin and Jurassic terrestrial sediments in the footwall of the Pengguan Fault (Chen & Wilson, 1996) (Fig. 2). The Upper Triassic foreland basin therefore extended a considerable distance northwest of the present-day front of the Longmen Shan Thrust Belt. The latest activity on the Pengguan Fault must be post-Jurassic, although there may have been earlier movement. The Tangwangzhai Nappe is believed to be a thin-skinned fold-thrust belt that stripped the shallow water Devonian–Upper Triassic cover from its Mesoproterozoic basement. To the southwest, the Tangwangzhai Nappe is represented by klippen of identical folded and thrusted Devonian–Upper Triassic carbonate (Fig. 2).

Guanxian-Anxian Nappe contains pre-Indosinian marine sedimentary rocks overlain by carbonate, shale, and sandstone of the Upper Triassic Xujiahe Group, deformed into SE-verging folds. The rocks in the footwall of the Guanxian-Anxian Fault are as young as Cretaceous (Chen & Wilson, 1996). This nappe is therefore essentially composed of deformed and uplifted foreland basin rocks (Fig. 2).

The Longmen Shan Foreland Basin

The Longmen Shan Foreland Basin, which lies on the western flank of the South China Block, consists of < 10 km of Upper Triassic to Quaternary strata (Watson *et al.*, 1987; Li *et al.*, 1995) (Fig. 3). The geological evolution of the western flank of the South China Block can be divided into three major stages: (i) a cratonic-passive margin stage characterised by the deposition of platform carbonates on the western South China Block during Sinian to Middle Triassic time, with important basaltic volcanism in the Late Permian (Luo *et al.*, 1990), (ii) a Late Triassic foreland basin stage characterised by predominantly marine to continental siliciclastic sedimentation and (iii) a terrestrial foreland basin or intracratonic stage from the Jurassic to Quaternary. In this study we focus on the Upper Triassic (Indosinian) foreland basin megasequence.

The Upper Triassic stratigraphy in the Longmen Shan Foreland Basin has been divided by Chinese workers into three formations in the western part, comprising the Maantang Formation (T_{3m}), Xiaotangzi Formation (T_{3xt}) and Xujiahe Formation (T_{3x}). In Chinese lithostratigraphy, the Xiaotangzi Formation (T_{3xt}) is equivalent to the first member of the Xujiahe Formation (T_{3x}^{1}). The Xujiahe Formation has been further divided into four members labelled T_{3x}^{2}, T_{3x}^{3}, T_{3x}^{4} and T_{3x}^{5}. The initiation of Indosinian foreland basin sedimentation can be traced to the deposition of Upper Triassic (Carnian, commencing at c. 227 Ma, Gradstein *et al.*, 1995) carbonate of the Maantang Formation (T_{3m}) and continued until the end of the Triassic (Rhaetian, ending at c. 206 Ma). The maximum duration of the Indosinian foreland basin megasequence is therefore c. 21 Myr.

Although there is clearly some merit in retaining existing lithostratigraphic schemes found in Chinese literature, the existing stratigraphic breakdown does not reflect (nor illuminate) the tectonic controls on foreland basin deposition during the Indosinian Orogeny (see Section 'Tectonostratigraphic Units of the Upper Triassic Longmen Shan Foreland Basin Fill'). A comparison of existing stratigraphic usage and the informal scheme used in this paper is given in Table 1.

In the following sections, we make use of a compilation of data on stratigraphic thicknesses, biostratigraphy, seismic facies, palaeocurrents and sedimentary petrography, largely previously published in the Chinese language literature. General information on the sedimentary geology of the Upper Triassic of the Longmen Shan Foreland

Table 1. Stratigraphy of the Indosinian foreland basin megasequence of the Longmen Shan Foreland Basin.

Chinese stratigraphic scheme (Li *et al.*, 1995)	Equivalent units of Chen *et al.* (1995)	Scheme used in this paper	Notation	Age (Ma) Gradstein *et al.* (1995)
Xujiahe Formation		Xujiahe Group		
Fifth Member	T_{3x}^{3}	Fifth Formation	T_{3x}^{5}	Rhaetian $205.7 \pm 4.0 - 209.6 \pm 4.1$
Fourth Member		Fourth Formation	T_{3x}^{4}	
Third Member	T_{3x}^{2}	Third Formation	T_{3x}^{3}	Norian $209.6 \pm 4.1 - 220 \pm 4.4$
Second Member	T_{3x}^{1}	Second Formation	T_{3x}^{2}	
First Member = Xiaotangzi Fm.		First Formation = Xiaotangzi Fm.	$T_{3x}^{1} = T_{3xt}$	
Maantang Formation		Maantang Formation	T_{3m}	Carnian $220 \pm 4.4 - 227 \pm 4.5$

Basin is found in the Regional Geology of Sichuan Province (1991) and the Regional Geological Map and Report of Longmen Shan (1995). More specific information on stratigraphic thicknesses, which form the basic data for the construction of isopach maps, comes from outcrop studies (Liu & Zhou, 1982; Li *et al.*, 1995; Lin *et al.*, 1996), and from boreholes and seismic stratigraphy (Hu & Yan, 1987; He, 1989). Biostratigraphic information is found in Liu & Zhou, (1982), Deng *et al.* (1982), Yang (1982) and Lin *et al.* (1996). The lithofacies of the Upper Triassic, including petrographic and provenance studies, have been interpreted by Liu & Zhou (1982), Deng *et al.* (1982), Shu *et al.* (1988), Li *et al.* (1995), Guo *et al.* (1996) and Lin *et al.* (1996). The seismic facies of the Upper Triassic have been interpreted by Hu & Yan (1987), He (1989) and Wang (1990). This Chinese language material will not be repeatedly cited in the descriptive sections that follow.

TECTONOSTRATIGRAPHIC UNITS OF THE UPPER TRIASSIC LONGMEN SHAN FORELAND BASIN FILL

Outcrop, borehole and seismic reflection data show that the Late Triassic Longmen Shan Foreland Basin has an asymmetric cross-sectional geometry thickening to the west (Fig. 2). The near-complete, thick (> 3 km) stratigraphic section in the west suggests high (c. 0.2 mm yr^{-1}) subsidence rates close to the western orogenic margin of the basin. The rate of subsidence and sediment accumulation at the western proximal margin of the Longmen Shan Foreland Basin is typical of the proximal parts of foreland basins as a generic basin type (Allen *et al.*, 1986).

The Upper Triassic foreland basin megasequence (*sensu* Hubbard *et al.*, 1985) is bounded by two major unconformities of regional extent; a basal unconformity between Middle and Upper Triassic, and an upper unconformity between Upper Triassic and Jurassic (Wang *et al.*, 1989). The dominant pattern of the megasequence at the proximal margin of the basin is of a sedimentary succession punctuated by a series of marine or lake flooding surfaces (laterally traceable in seismic profiles) and unconformities, separating coarsening-upward and fining-upward stratigraphic units. We identify three such tectonostratigraphic units in the Indosinian stage of the Longmen Shan Foreland Basin (Fig. 4).

Tectonostratigraphic unit 1

Tectonostratigraphic unit 1 is marked by early carbonate platform drowning and retrogradation at the distal (cratonic) margin, followed by a strong progradation from the proximal (orogenic) margin. It is composed of the Maantang Formation (T_{3m}), Xiaotangzi Formation (T_{3xt}) (which is equivalent to the first formation of the Xujiahe Group), and the Second Formation of the Xujiahe Group (T_{3x}^{2}) (Fig. 4, Table 1).

Maantang Formation (T_{3m})

The Maantang Formation is only found above the basal unconformity along the western fringe of the South China Block. It is mostly composed of marine black mudstone and shale, interbedded with siltstone, marl, oolitic and bioclastic limestone and sponge reefs. The biostratigraphic age of the Maantang Formation (based on ammonites, bivalves, foraminifera, corals, sponges, brachiopods, echinoids, crinoids and conodonts such as *N. eogondolella, N. polygnathiformis, N. navicula, N. jiangyouensis*) is Carnian (c. 227–220 Ma).

The basal boundary of the Maantang Formation is a major unconformity between Middle and Upper Triassic rocks, but with little or no angular discordance. It is also recognised as a seismic reflection boundary with truncation and onlap. In outcrop at Emei (Fig. 5), the unconformity is characterised by palaeokarst and evaporite-solution breccias. The basal unconformity cannot be recognised as a stratigraphic break throughout the foreland basin system. In the western part of the basin there is no discordance between Middle and Upper Triassic stratigraphy based on observations from boreholes. In the eastern part of the basin, however, there is better evidence from boreholes of a stratigraphic break between Middle and Upper Triassic, including bedrock-confined palaeokarst preserved along the unconformity surface. This indicates that the pre-Upper Triassic subcrop was exposed subaerially.

The Maantang Formation is composed of two parts. The lower part is made up of neritic mudstone, sandstone

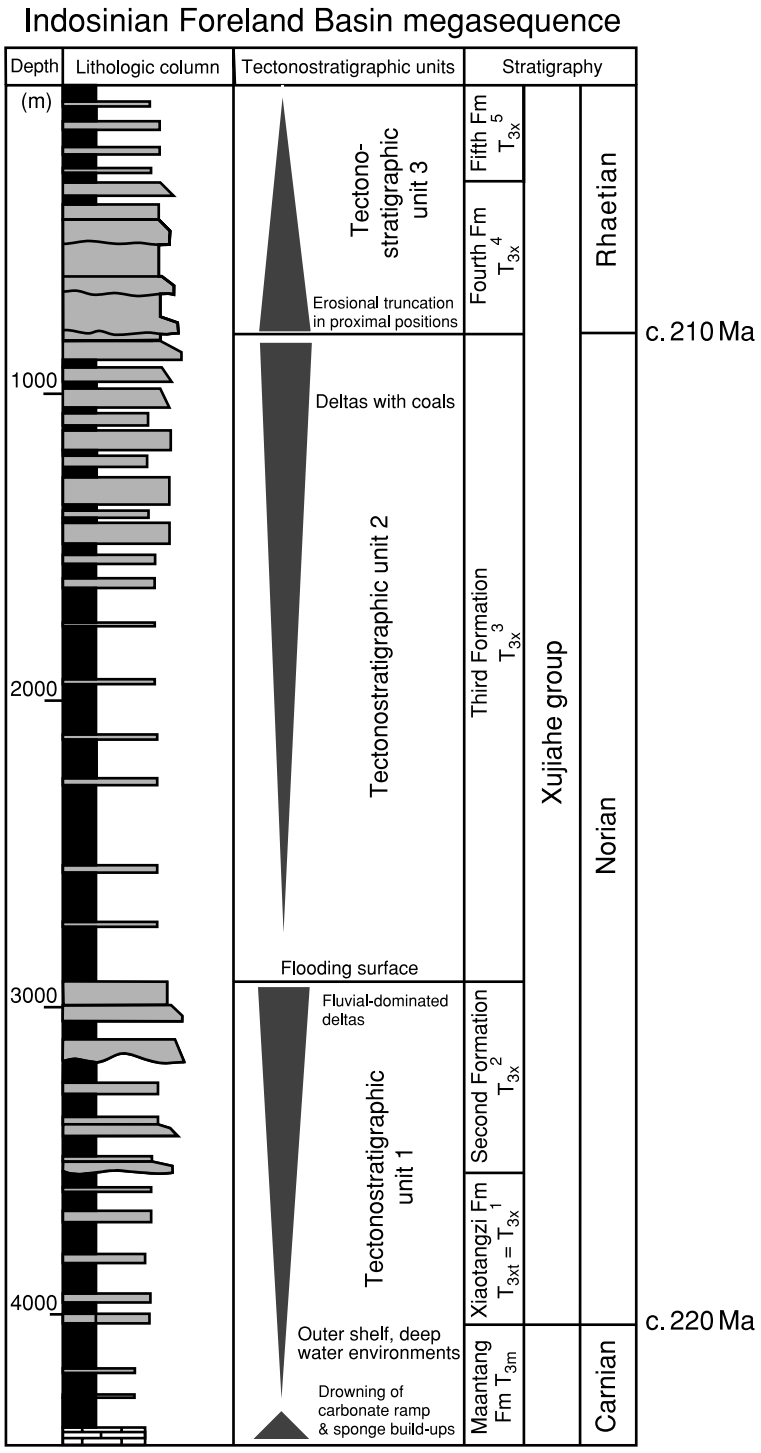

Fig. 4. Generalised sedimentological log of the foreland basin megasequence for a location close to the present trace of the Beichuan Fault, showing coarsening/fining trends, unconformities and flooding surfaces that collectively define tectonostratigraphic units 1–3. Ages of the Carnian–Norian and Norian–Rhaetian boundaries are taken from Gradstein *et al*. (1995).

and bioclastic limestone in an upward-fining succession. Carbonate shoal facies and patch reefs record the presence of a carbonate ramp. The basal early Carnian limestone of the Maantang Formation was deposited on a west-facing, NE–SW orientated carbonate ramp at the eastern, distal margin of the early foreland basin (Fig. 5). The carbonate ramp attains a thickness of 30–100 m and thins to the southeast. The patch reefs are composed of sponge bioherms at Hanwang, Mianzhu and Jiangyou. These sponge reefs have also been recognised by a mounded seismic reflection character (200–700 m relief) under sheet drape seismic facies. The lower part of the Maantang Formation bears strong resemblance to the distal margin carbonate-dominated facies developed in other foreland basins such as the European Alps (Crampton & Allen, 1995; Allen *et al*., 2001). The carbonate ramps are interpreted as photic zone build-ups drowned as flexural subsidence progressively increased at the cratonic margin of the basin (Dorobek, 1995; Galewsky, 1998; Allen *et al*., 2001). As in the Neoproterozoic *Namacalathus-Cloudina* reefs of

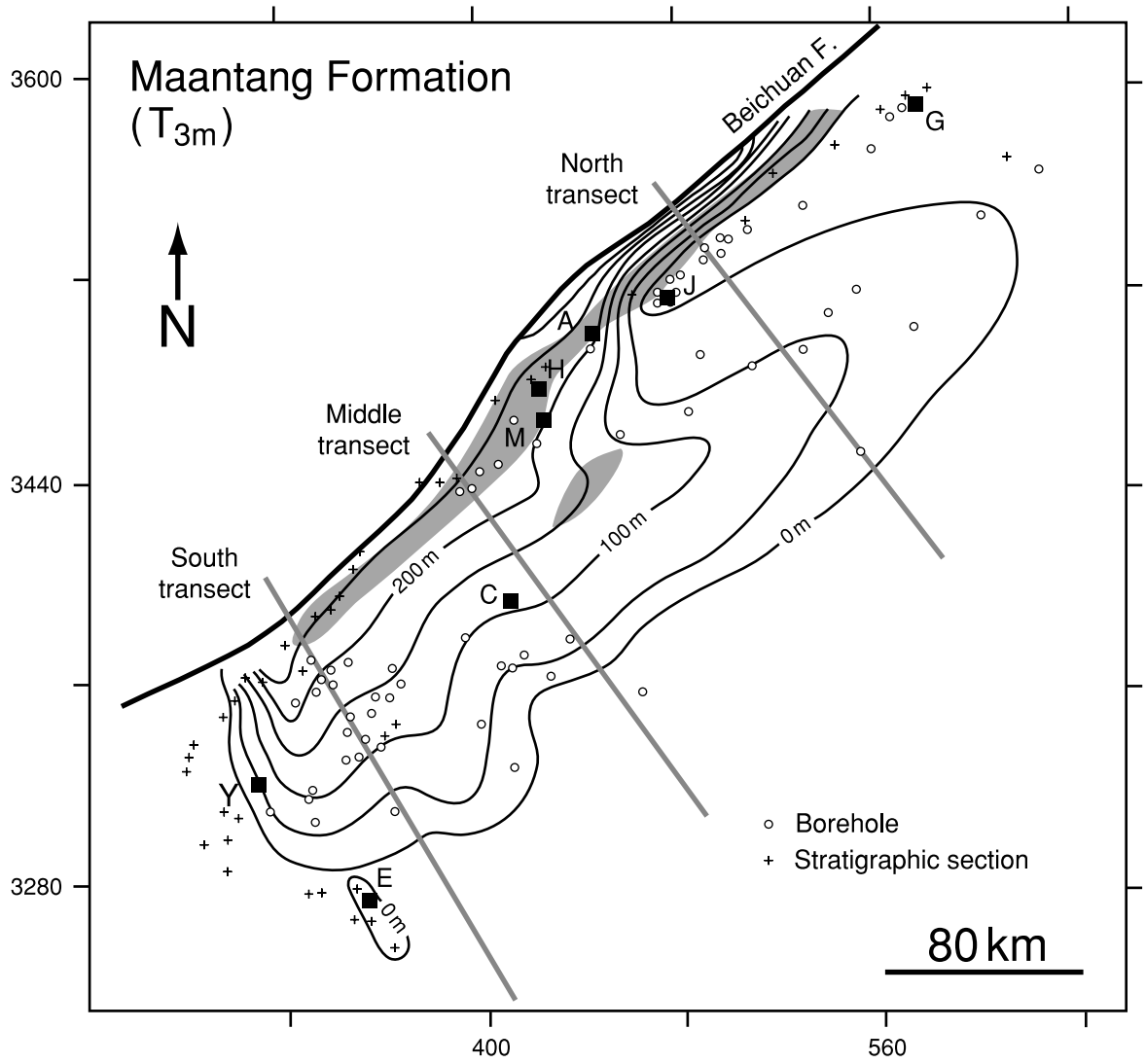

Fig. 5. Isopach and palaeogeographical map of the Maantang Formation (T_{3m}) based on boreholes (circles) and measured stratigraphic sections in outcrop (crosses). Contour interval 50 m. Heavy black line shows the approximate present-day trace of the Beichuan Fault. Grey lines show the locations of the three transects used in the flexural modelling (Figs 11–15). Light grey areas show the locations of carbonate banks and sponge reefs within the Maantang Fm. The early foreland basin deepened into deep-water environments close to, and probably west of, the present trace of the Beichuan fault. X and Y coordinates are in UTM, zone 48. Black squares show cities and locations mentioned in text: A, Anxian; C, Chengdu; E, Emei; G, Guangyuan; H, Hanwang; J, Jiangyou; M, Mianzhu; Y, Yaan.

the Nama Foreland Basin of Namibia (Saylor *et al.*, 1995), the sponge reefs developed high amplitudes in down-dip locations as accommodation outpaced sediment production, before eventual drowning and retrogradation.

The upper part of the Maantang Formation is composed of neritic siltstone, mudstone, sandstone and pyritic black shale interbedded with marl. The Maantang Formation therefore shows an overall fining and deepening upward (Fig. 4). The observable maximum thickness of the upper part of T_{3m} in boreholes is > 400 m in the west, thinning southeastward, so the geometry is wedge-shaped (Fig. 5). In a transverse section, there was a deep-water basin in the west, shoal facies and patch reefs on the edge of a carbonate ramp in the middle, and a shallow shelf in the eastern part. Provenance and palaeocurrent studies indicate a derivation of sediment from the east, which is the location of the presumed flexural forebulge. No detritus derived from the western orogenic margin can be discerned at this time. The western edge of the basin cannot be well constrained, but is likely to have been situated to the northwest of the palinspastically restored position of the Beichuan Fault. Assuming shortening by a factor of ~2 in the Guanxian-Anxian Nappe, as estimated from available cross-sections (e.g. Burchfiel *et al.*, 1995; Chen & Wilson, 1996), this basin margin was at least 70 km northwest of the present position of the Pengguan Fault, which marks the front of the Longmen Shan Thrust Belt.

Xiaotangzi Formation (T_{3xt})

The Xiaotangzi Formation (equivalent to the first formation of the Xujiahe Group, T_{3x}^{1}), is composed of black

marine shale, mudstone, quartz arenite, lithic arenite and siltstone, and can be divided into three parts: the lower part is composed of black shale interbedded with quartz arenite, the middle part comprises lithic arenite and black shale, and the upper part is composed of arkose. The Xiaotangzi Formation coarsens upwards and is thought to represent a transition from marine shelf to delta environments. It is early Norian in age on the basis of its fossil content: plants such as *Thaumatopteris* sp., *Lepidopteris* sp., *Clathropteris meniscioides*, bivalves (*Burmesia lirata* Healey, *Halobia* cf. *fallax* Mojs, *Myophoria* (*Costatoria*) *seperata, Pteria krumbecki, Myophoria seperata*) and spores (*Protoanemitee, Taeniaesporites, Discisporites*).

Quartz arenites (1–30 m thick) occur above a basal flooding surface. These strata contain ubiquitous soft sedimentary deformation structures indicative of an unstable prodelta slope. At Guangyuan, Jiangyou, Anxian and Emei, the formation is made of black shale interbedded with coal, lithic arenites and siltstones, indicating delta top environments.

The maximum observed thickness of T_{3xt} is > 550 m in the west, gradually thinning southeastward (Fig. 6). The depocentre was probably located in the northwestern part of the basin, and migrated southeastward relative to the depocentre of the Maantang Formation. The provenance of clasts in the sandstones and conglomerates indicates two source areas, including the orogenic margin (Songpan-Ganzi Fold Belt) as well as the cratonic forebulge margin.

The Second Formation of the Xujiahe Group (T_{3x}^{2})

The Second Formation of the Xujiahe Group is composed of a coarsening- and shallowing-upward succession recording the progradation of a delta system into a lacustrine basin (Fig. 4), indicating that the basin had now lost

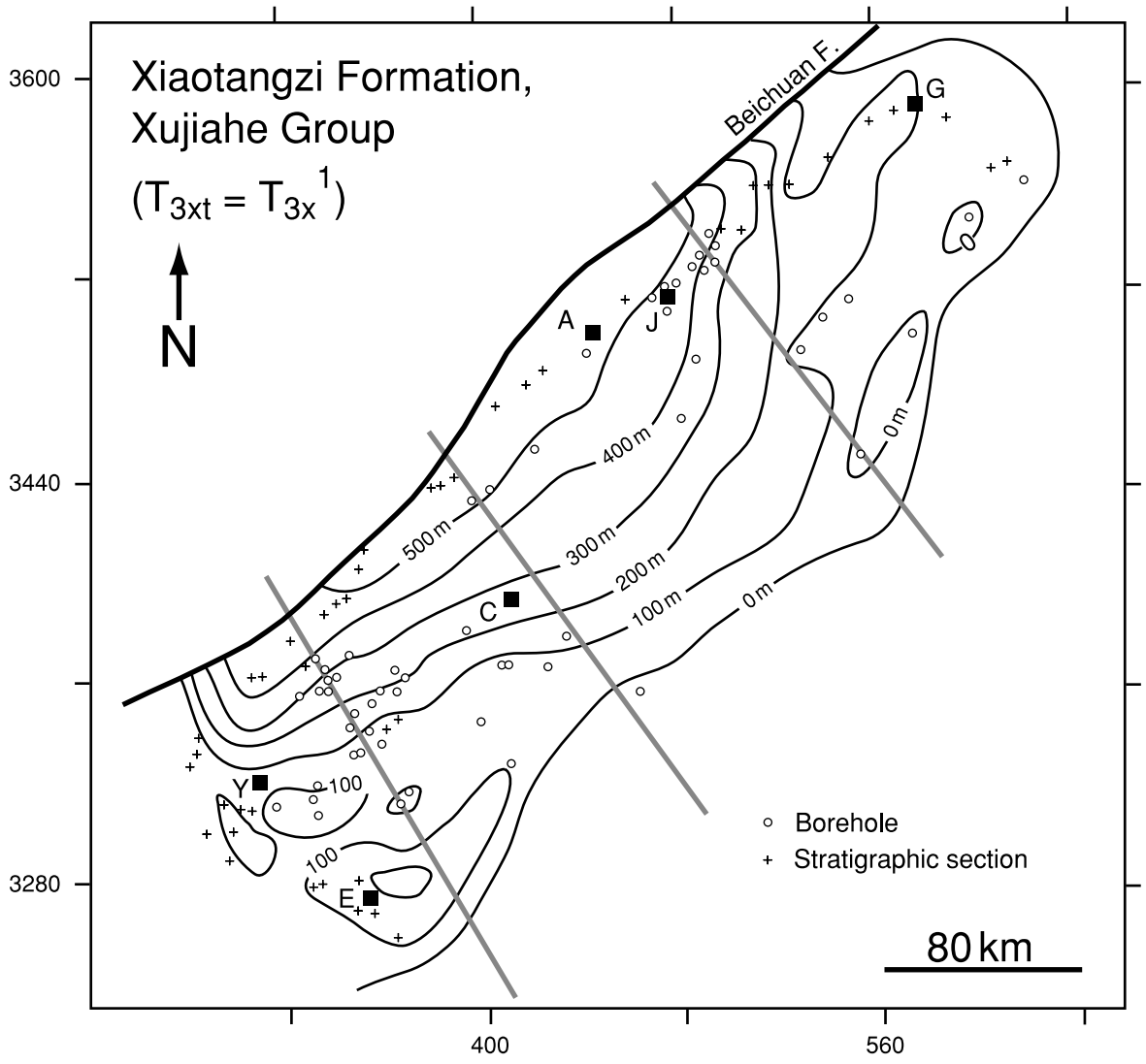

Fig. 6. Isopach map of the Xiaotangzi Formation (T_{3xt}), equivalent to the lowermost formation of the Xujiahe Group (T_{3x}^{1}), based on boreholes (circles) and measured stratigraphic sections (crosses). Littoral facies along the forebulge margin passed laterally into prodelta sediments in the foredeep. Contour interval 100 m. Symbols as in Fig. 5.

its connection to the open sea. The sediments comprise sandstone interbedded with conglomerate, siltstone and mudstone. T_{3x}^{2} can be divided into three parts. The lower part is composed of lithic arenite and arkose interbedded with conglomerate. The middle part is composed of lacustrine black shale interbedded with siltstone, and the upper part comprises lithic arenite, arkose and conglomerate.

The maximum observable thickness is >800 m in the west, gradually thinning southeastward (Fig. 7). A braidplain delta system existed in a facies tract situated along the present front of the Longmen Shan Thrust Belt, with a lacustrine system in the eastern part of the foreland basin. The age of the Second Formation of the Xujiahe Group is middle Norian on the basis of its fossil content, including plants (*Dictyophllum nathorsti* Zeiller, *Lepidopteris ottonis*) and bivalves (*Unionites* sp., *Taneredia garandi* Mansuy, *Cardita* (*Palaeocardita*) *singularis* Healey, *Burmesia* sp., *Krumbeckia* sp.).

The provenance of clasts and palaeocurrents in the sandstone and conglomerate indicate just one source area in the Songpan-Ganzi Fold Belt. Through tectonostratigraphic unit 1 therefore, there was a gradual switch from craton-derived to orogen-derived siliciclastics linked to a progradation of orogenic sources, combined with a general southeasterly migration of the basin.

Tectonostratigraphic unit 2

Tectonostratigraphic unit 2 is composed of the Third Formation of the Xujiahe Group (T_{3x}^{3}). The lower boundary is marked by a lake flooding event recognised as a major facies change in many stratigraphic sections and as an important seismic reflection boundary associated with southeastward onlap in the subsurface of the foreland basin. The age of the tectonostratigraphic unit is late Norian on the basis of its fossil content, including plants (*Clathropteris meniscoides* Brongn, *Pterophyllum chinense*

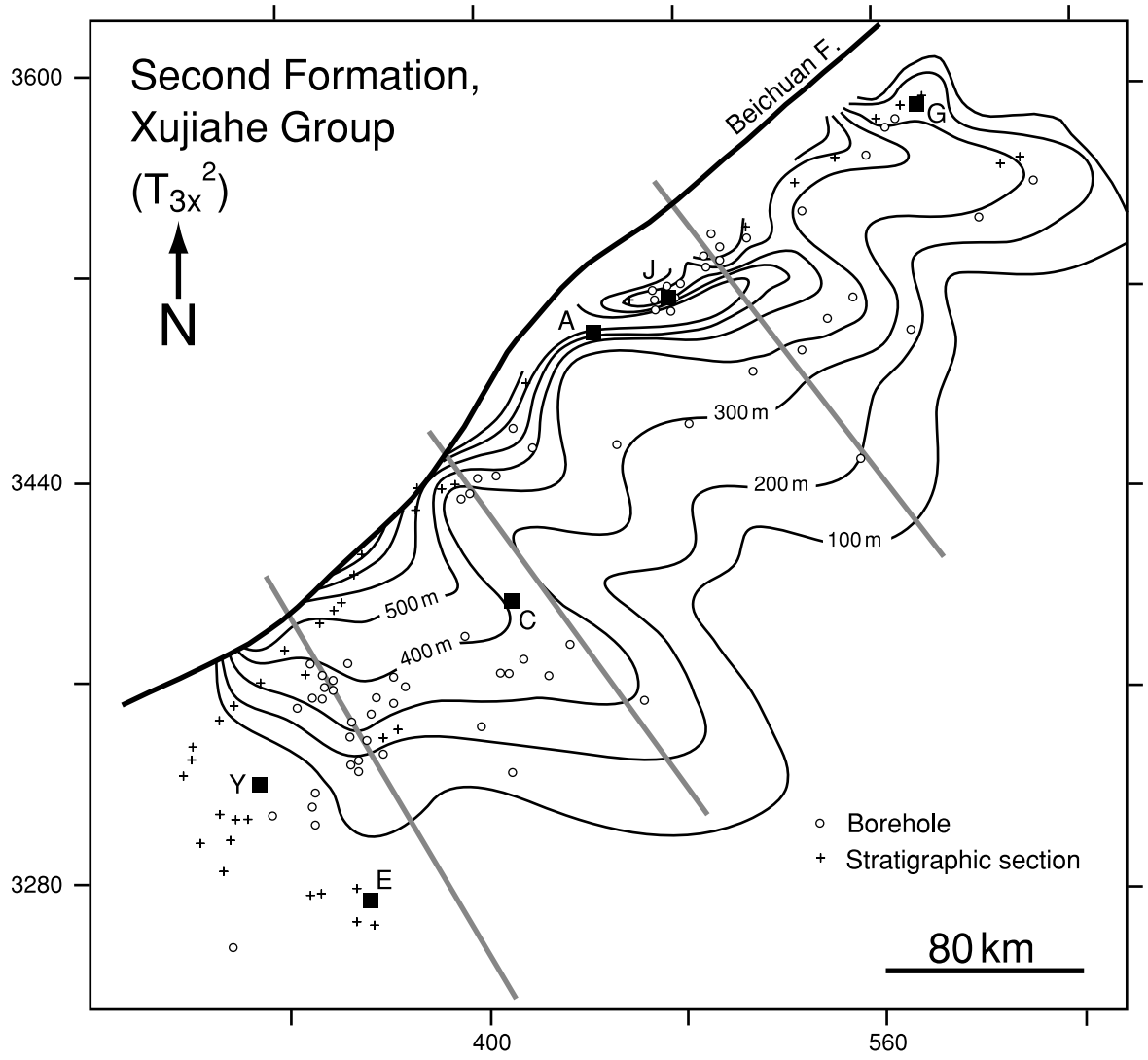

Fig. 7. Isopach map of the Second Formation of the Xujiahe Group (T_{3x}^{2}), based on boreholes (circles) and measured stratigraphic sections (crosses). Deltaic progradation took place from the northwesterly orogenic margin. Contour interval 100 m. Symbols as in Fig. 5.

Li, *Neocalamitas hoyiewanensis*, *Podozamites lanceolatus*, *Equisetites* cf. *acantodon*), spores (*Ricciisporites tuberculatus* Lundblad, *Zebra sporites*) and bivalves (*Modiolus waiyuanensis* Gu).

Tectonostratigraphic unit 2 is made of black shale, mudstone, lithic arenite, siltstones, conglomerate and coal in an overall upward-coarsening succession. The lower part of T_{3x}^3 is composed of black shale interbedded with sandstone and siltstone. The upper part is composed of sandstone, conglomerate and interbedded shale, and shows a shallowing-upward into lacustrine delta and stream channel environments (Fig. 4).

The maximum observable thickness is >1750 m in the west, gradually thinning southeastward (Fig. 8). In a NW–SE transverse section, a delta system occupied a facies tract located along the present-day front of the thrust belt, with a centrally located lacustrine system and minor delta system along the eastern margin of the foreland basin. Provenance and palaeocurrent studies indicate that the sediments were derived from both the Songpan-Ganzi Fold Belt and the forebulge region of the South China Block.

Tectonostratigraphic unit 2, therefore, was initiated by a major lake flooding, associated with a southeasterly onlap of the distal (cratonic) margin of the basin. Sedimentation proceeded through major deltaic progradation from the orogenic margin and minor sediment input from the cratonic margin into a centrally located lake. The abrupt facies discontinuity signifying a deepening of water depths marking the base of tectonostratigraphic unit 2 may be due to loading events in the orogenic hinterland causing renewed phases of flexural subsidence (Flemings & Jordan, 1989; Sinclair *et al.*, 1991). If so, the shallowing up that follows represents either tectonic or sedimentary progradation following a rapid increment of flexural subsidence.

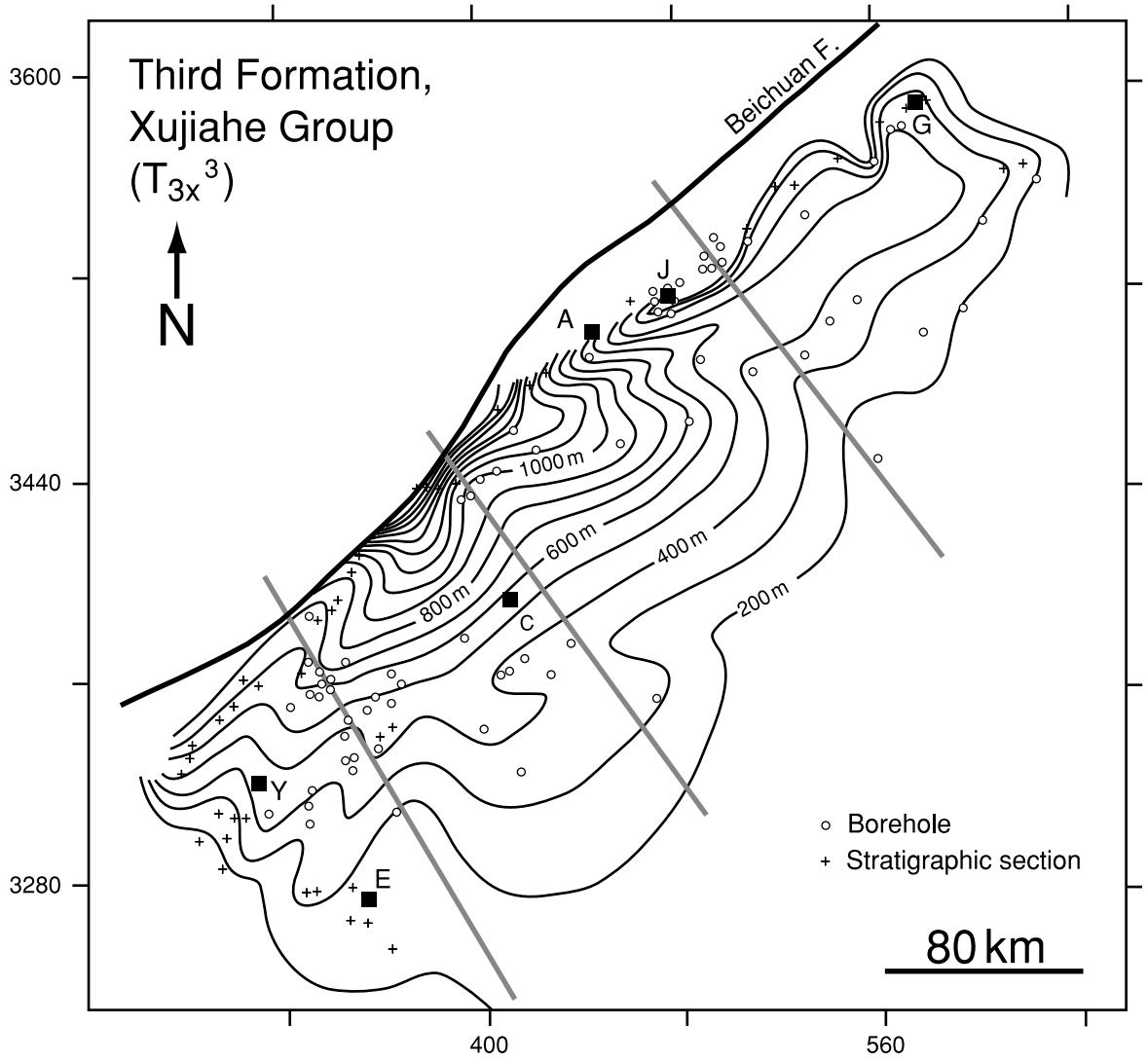

Fig. 8. Isopach map for the Third Formation of the Xujiahe Group (T_{3x}^3) based on boreholes (circles) and measured stratigraphic sections (crosses). Contour interval 100 m. Symbols as in Fig. 5.

Tectonostratigraphic unit 3

Tectonostratigraphic unit 3 comprises the Fourth (T_{3x}^4) and Fifth (T_{3x}^5) Formations of the Xujiahe Group. The lower boundary is an unconformity in the proximal margin of the foreland basin (Li *et al*., 1995) and clearly shows truncation and westward onlap in the seismic reflection section (Wang, 1990). The upper boundary is a major angular unconformity between Triassic and Jurassic rocks at outcrop (Li *et al*., 1995) and in seismic reflection sections in the Longmen Shan Foreland Basin. The age of tectonostratigraphic unit 3 is Rhaetian based on the non-marine fossil content including plants (*Podozamites lanceolatus*, *Neocalamites carcinoides*, *Neocalamites carrerei*, *Equisetites* cf. *Carrani*) and spores (*Dictyophyllidites*, *Clathroidites*, *Cadargasporites*, *Kyrtamisporis*).

Tectonostratigraphic unit 3 is a fining-upward succession that can be divided into two parts. The lower part is a fluvial fan or fan delta composed of debris-flow conglomerate interbedded with sandstone and black shale; the lacustrine upper part is composed of black shale interbedded with siltstone and sandstone. Relative to the underlying rocks, tectonostratigraphic unit 3 represents a regressive sequence distributed throughout the Sichuan Basin (Fig. 4). Palaeogeographically, a system of fan deltas in the northwest of the basin passed southeastwards into a lacustrine system.

The maximum observable thickness is >1000 m in the west of the basin, thinning to the southeast (Figs 9 and 10). Clasts of metamorphic and carbonate rocks containing abundant fossils indicate that the sediments could only have been derived from the Songpan-Ganzi Fold Belt and from the Jiuding Shan Nappe and the Pengxian-Guanxian Basement Complex of the Longmen Shan Thrust Belt.

Tectonostratigraphic unit 3, therefore, records major southeasterly progradation from the orogenic margin of the basin associated with strong westward stratigraphic onlap of the basin margin to produce an extensive sedimentary sheet. The unconformity at the base of tectonostratigraphic unit 3, recognised as a truncation in seismic

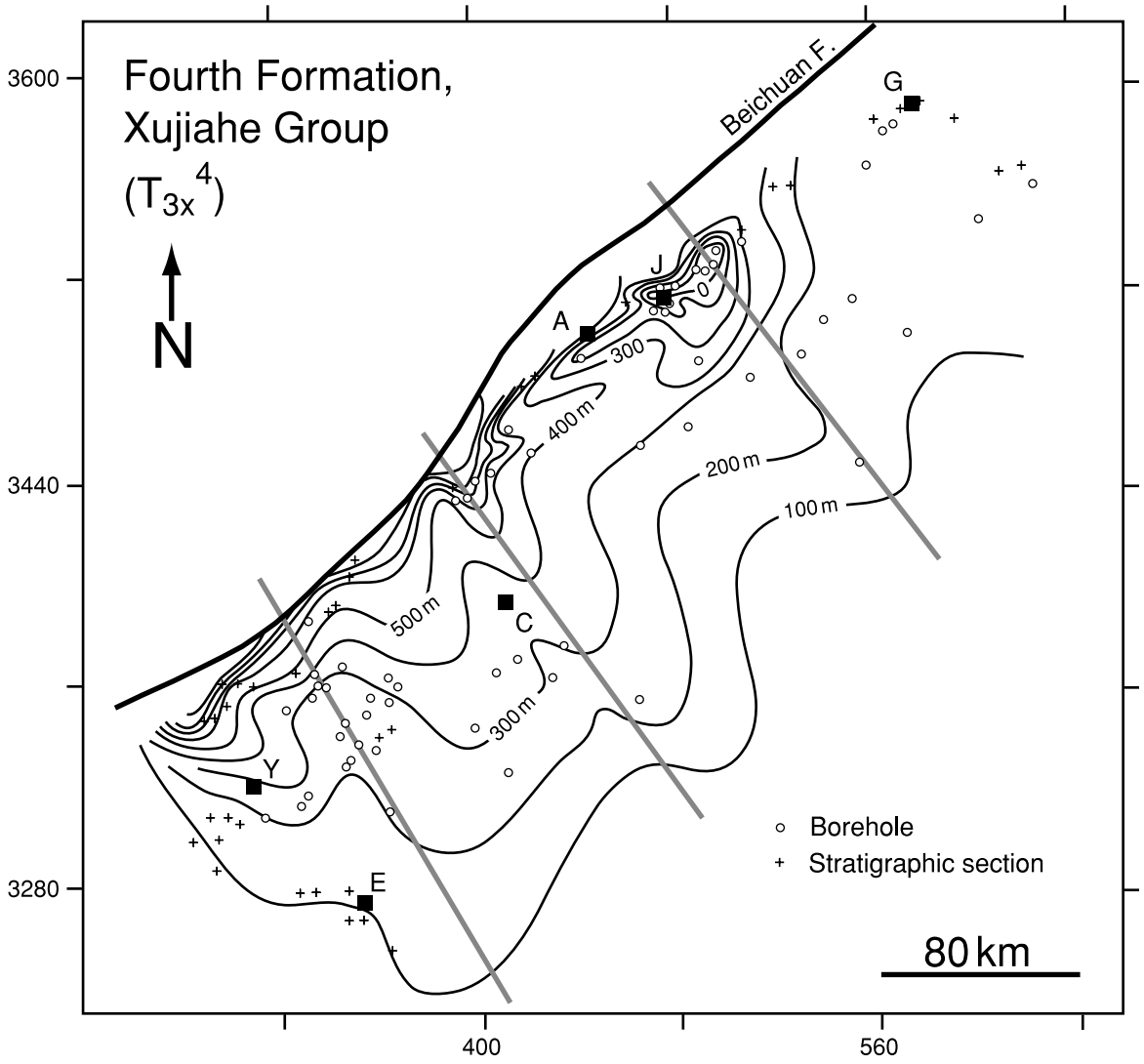

Fig. 9. Isopach map of the Fourth Formation of the Xujiahe Group (T_{3x}^4) based on boreholes (circles) and measured stratigraphic sections (crosses). Locally developed fan-deltas existed in the northwest of the basin. Contour interval 100 m. Symbols as in Fig. 5.

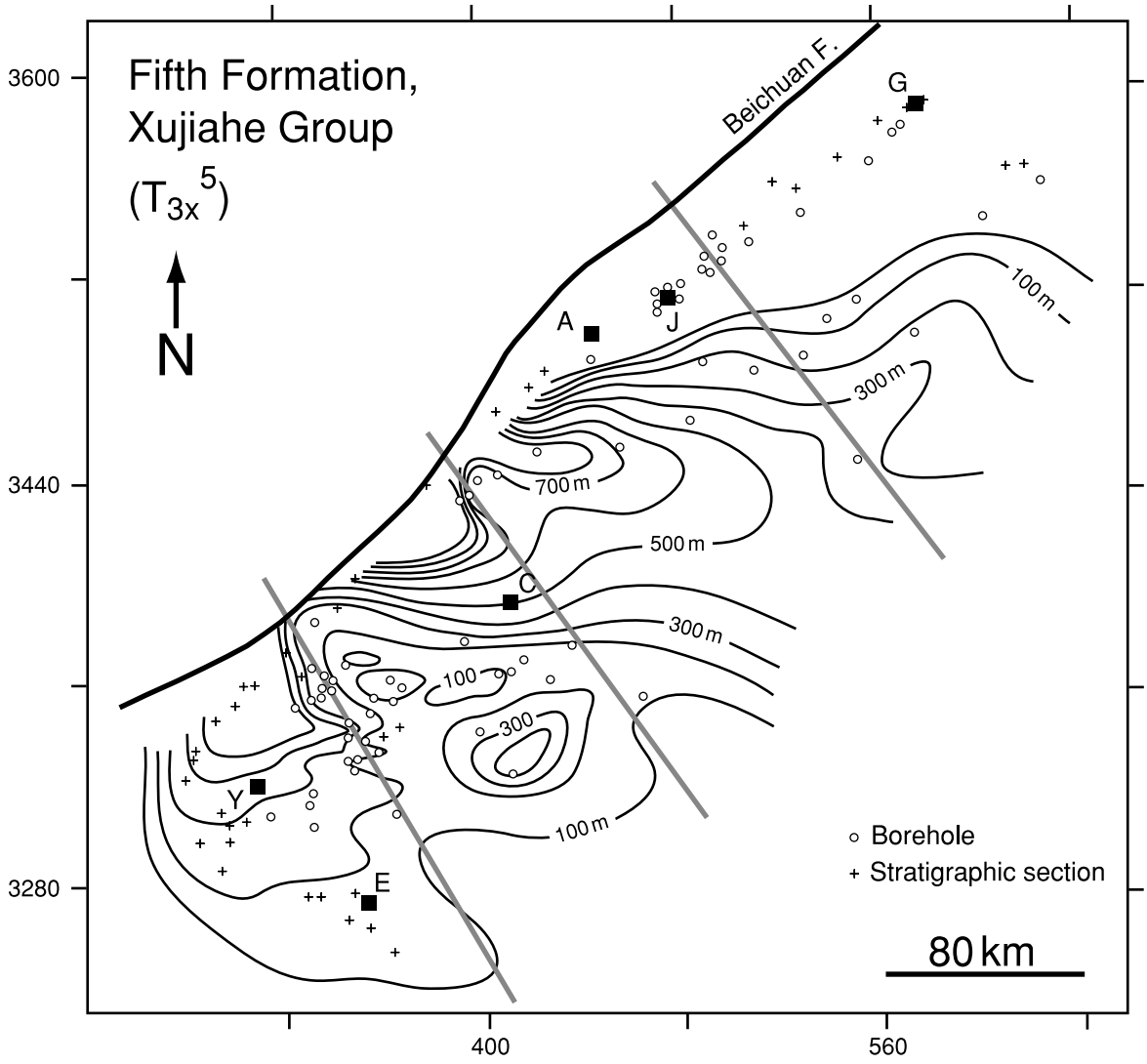

Fig. 10. Isopach map of the Fifth Formation of the Xujiahe Group (T_{3x}^5) based on boreholes (circles) and measured stratigraphic sections (crosses). Contour interval 100 m. Symbols as in Fig. 5.

reflection profiles between the Third (T_{3x}^3) and Fourth (T_{3x}^4) Formations of the Xujiahe Group (Wang, 1990; Li *et al.*, 1995), is only developed at the proximal basin margin. Its formation may be linked to crustal uplift over blind thrust faults (e.g. Martin-Martin *et al.*, 2001) or to isostatic rebound during times of tectonic quiescence (Heller *et al.*, 1988).

Underfilled and overfilled condition of the Longmen Shan Foreland Basin

The upward transition from an underfilled deep water or 'flysch' stage to an overfilled shallow marine and continental or 'molasse' stage has been recognised as a distinctive and important evolutionary pathway of many foreland basins (Miall, 1978; Covey, 1986; Homewood *et al.*, 1986; Sinclair & Allen, 1992). The underfilled and overfilled stages represent very different balances between flexural subsidence, tectonic progradation and sediment flux and result in fundamentally different depositional systems and drainage patterns, basin architecture and subsidence rates.

The sedimentary style of the Maantang Formation is predominantly deep marine shale and mudstone, suggesting that the basin was underfilled at this stage. The underfilled status continued through the Deposition of the shale and siltstone dominated Xiaotangzi Formation, with a dual sediment supply. The bulk of the sediment was derived from the Longmen Shan Thrust Belt, with a subordinate supply from the forebulge. The Longmen Shan Foreland Basin, therefore, has striking similarities with the underfilled trinity of the European Alps (Sinclair, 1997) during the deposition of the Maantang (T_{3m}) and Xiaotangzi (T_{3xt}) Formations.

During the deposition of the Second Formation of the Xujiahe Group (T_{3x}^2), the predominance of deltaic sandstones indicates that the basin was approaching an overfilled condition. The only recognizable detrital sediment supply is from the Longmen Shan Thrust Belt. The basin became separated from the open ocean.

During the deposition of tectonostratigraphic units 2 and 3, major delta and fluvial systems fed sediment from the Longmen Shan Thrust Belt into a foreland basin with a centrally located lake. The predominance of fluvial sandstones and conglomerates in tectonostratigraphic unit 3 shows the basin to have been in an overfilled condition. The change from an underfilled to an overfilled basin reflects the interplay between wedge advance rate, taper angle of the orogenic wedge, flexural rigidity of the underlying plate and the sediment efflux of the mountain belt. In the Tertiary North Alpine Foreland Basin, Allen *et al.* (1991) and Sinclair & Allen (1992) suggested that the key factor in explaining the 'flysch-molasse transition' was a slowing down of the advance rate of the orogenic wedge combined with higher topography driving larger sediment fluxes into the basin. Schlunegger (1999) and Schlunegger *et al.* (2001) have emphasised the climatic changes accompanying and possibly driving changes in sediment flux to the North Alpine Foreland Basin.

Basal unconformity and wedge advance rate

The basal unconformity of foreland basin megasequences is typically cut by the migration of an uplifted forebulge region across the foreland plate (Jacobi, 1981; Quinlan & Beaumont, 1984; Coakley & Watts, 1991; Crampton & Allen, 1995; Allen *et al.*, 2001). The passage from an unconformity to a lateral conformity is one of the features of flexural forebulge unconformities described and modelled by Crampton & Allen (1995) from the base of the North Alpine Foreland Basin in Switzerland. The basal unconformity between the underlying Palaeozoic–Middle Triassic passive margin and the Upper Triassic Longmen Shan Foreland Basin is a good candidate for a flexural forebulge unconformity.

If the assumption is made that the basal unconformity was cut during subaerial emergence in a flexural forebulge region, the present-day geometry of this surface gives an indication of the convergence between the South China foreland and the Longmen Shan Thrust Belt since the initiation of the unconformity at the beginning of T_{3m} (Maantang Formation) time. The unconformity becomes a conformity in the region of Anxian, which is c. 10 km from the present-day trace of the Beichuan Fault. In a transverse direction, this position is approximately 120 km from the pinch-out of youngest Maantang Formation, and approximately 180 km from the pinch-out of youngest Xujiahe Group (T_{3x}^{5}). This indicates that the migration rate of the orogenic wedge (assuming a constant geometry) early in foreland basin history (c. 227–220 Ma) was rapid (c. 15 mm yr^{-1}) compared to the slow migration rate (maximum of 5 mm yr^{-1}) during the remainder of foreland basin evolution (Xujiahe Group, c. 220–206 Ma). This marked slowing of the migration rate of the orogenic wedge is supported by the modelling results presented below.

Dorobek (1995) and Allen *et al.* (2001) have shown how the preserved stratigraphic thickness of distal foreland basin carbonate ramps depends on a number of factors including flexural rigidity, load migration rate, carbonate productivity rate and eustatic effects. The stratigraphic thickness of the basal carbonate of the Maantang Formation is 30–100 m. Using Allen *et al.*'s (2001) numerical model, such thicknesses can be explained by either a combination of a rigid plate ($Te > 25$ km) and fast load migration rate (c. 12 mm yr^{-1}) or a weak plate ($Te < 15$ km) and slow load migration rate (c. 4 mm yr^{-1}). Since our modelling results given below require a relatively rigid plate, we once again infer a fast load migration rate of >10 mm yr^{-1} during the initial stage of foreland basin development.

FLEXURAL MODEL OF THE LONGMEN SHAN FORELAND BASIN

Model description

It is now a standard procedure in basin analysis to model the subsidence in foreland basins as due to the emplacement of tectonic loads on an elastic plate (Jordan, 1981; Turcotte & Schubert, 1982; Stockmal & Beaumont, 1987; Watts, 1992). In reality, such tectonic loads may be complex spatially and temporally variable (Flemings & Jordan, 1990; Sinclair *et al.*, 1991; Whiting & Thomas, 1994; DeCelles & Mitra, 1995), the underlying lithosphere may have spatially and temporally variable strength (Beaumont, 1981; Stewart & Watts, 1997; Cardozo & Jordan, 2001), and surface process systems may result in very wide variations in the spatial patterns and fluxes of sediment delivery to foreland basins as a function of climate, bedrock types and exhumation patterns (Johnson & Beaumont, 1995; Schlunegger & Willett, 1999; Schlunegger, 1999; Kühni & Pfiffner, 2001). Despite these complexities, there is some merit in using basin stratigraphic thicknesses and gross depositional environments, as well as palinspastic positions of thrust fronts and basin margin facies, to generate a plausible set of values of geodynamic parameters at the time of foreland basin development. We have therefore used a one-dimensional analytical model of a discrete assemblage of tectonic loads (Jordan, 1981) flexing down an infinite elastic plate (Hetenyi, 1946) in three NW–SE transects across the Longmen Shan Thrust Belt and Foreland Basin. The algorithms used can be found in Jordan (1981).

Three load configurations are modelled corresponding to the times at the close of deposition of each of the three tectonostratigraphic units. Crustal loads are assumed to have a uniform density of $\rho_c = 2700$ kg m^{-3} and to displace an underlying mantle with density $\rho_m = 3300$ kg m^{-3}. The sediment loads are estimated from sediment thicknesses in the foreland basin. The average bulk density $\overline{\rho_b}$ of basin-filling sediment, with water-filled porosity ϕ, depends on grain density ρ_{sg}, surface porosity ϕ_0 and maximum burial depth y (Athy, 1930; Allen & Allen, 1990):

$$\overline{\rho_b} = \rho_{sg}(1 - \phi) + \rho_w\phi \quad (1)$$

where $\phi = \phi_0 \exp(-cy)$, and c is a depth-porosity coefficient (Sclater & Christie, 1980). Using values of

parameters for a sandstone-shale mixture, which typifies the stratigraphy of the Longmen Shan Foreland Basin ($c = 0.4$, $\phi_0 = 0.5$, $\rho_{sg} = 2680\,kg\,m^{-3}$), estimated average bulk densities of the sedimentary fill vary from 2117 to $2510\,kg\,m^{-3}$ for maximum burial depths of 1–4 km, respectively. The average bulk density used in each model run is given in Table 2.

For each model run, the configuration of load blocks is constrained in part by the preservation of foreland basin stratigraphy in the Longmen Shan Thrust Belt. We make the following inferences: until T_{3x}^{3} time the foreland basin extended westwards at the very least to the palinspastically restored position of the Beichuan Fault, and possibly as far west as the Maowen Fault. This is consistent with the preservation of folded T_{3x}^{3} sedimentary rocks in the footwall of the Beichuan Fault (Chen & Wilson, 1996), and implies that the Tangwangzhai Nappe is a truly synsedimentary Indosinian feature. The preservation of $T_{3x}^{4,5}$ strata in the footwall of the Pengguan Fault (Chen & Wilson, 1996) suggests that activity on this structure accompanied or post-dated $T_{3x}^{4,5}$ deposition.

The deflection y caused by the different load configurations is mapped in the horizontal coordinate x from 0 to 300 km. At time A, corresponding to the end of deposition of tectonostratigraphic unit 1, we place the southeast margin of the crustal load system at $x = 120$ km, at the palinspastically restored position of the Beichuan Fault. At time B, after deposition of tectonostratigraphic unit 2, we allow the thrust front to propagate forward to $x = 140$ km. At time C, after deposition of tectonostratigraphic unit 3, the thrust front is at $x = 160$ km, at the position of the Pengguan Fault. At each time, the isostatically compensated crustal load blocks produce a model mountain belt topography that can be compared with present-day maximum heights and average slopes of mountain fronts. Mean slopes derived from 50 to 100 km-wide swaths vary from 0.014 to 0.049 with an average of 0.028 in the 10 examples shown in Table 2. Second, the isostatically compensated sediment load blocks generate a basin topography or bathymetry that can be compared with the water depths inferred from the gross depositional environments of the foreland basin fill. The crustal load configuration can therefore be modified in order to simulate reasonable mountain belt and basin topographic profiles. However, the key parameter that was varied in order to obtain reasonable mountain and basin topographic profiles was the flexural rigidity. We ran the analytical model along three transverse profiles using the load configurations given in Table 3 and a range of flexural rigidities from 10^{22} to 10^{24} N m, equivalent to elastic thicknesses from close to Airy isostasy up to 54.4 km (assuming $E = 70$ GPa, $v = 0.25$). An illustration of the sensitivity of model results to variations in flexural rigidity is given in Fig. 11.

Model results

At time A, after deposition of tectonostratigraphic unit 1, crustal load blocks are positioned between $x = 0$ and 120 km (Figs 11 and 12). Sediment load blocks are taken from isopach data along three transects in the north, middle and south of the basin (Fig. 12). Reasonable topographic profiles with mountain belt slopes of approximately 0.03 and shallow marine conditions in the basin can be generated with a flexural rigidity of 5×10^{23} N m (Te of ~43 km) (Fig. 12). There are no significant along-strike variations between the three transects at time A.

At time B, crustal load blocks are positioned between $x = 0$ km and $x = 140$ km (Fig. 13). This load configuration represents a significant thickening of the orogenic wedge compared to Time A, with a frontal advancement of just 20 km. The most satisfactory topographic profiles are generated with flexural rigidities in the range 5×10^{23}–5×10^{24} N m (Te of 43–54 km) in the three transects. The mountain belt average slope is approximately 0.03 for this combination of flexural rigidity and load configuration. There are significant differences in the model depositional profiles between the three transects (Fig. 13). In particular, the northern transect, which has much smaller thicknesses of tectonostratigraphic unit 2, shows deep proximal palaeobathymetry compared to the middle and southern transects.

At time C, the crustal loads are moved over the foreland as far as $x = 160$ km, representing a further 20 km of tectonic progradation compared to Time B (Fig. 14). Reasonable average mountain belt slopes (~0.025) and depositional profiles are obtained with flexural rigidities in the range 5×10^{23}–5×10^{24} N m (Te of 43–54 km). In the southern transect, proximal subaerial and distal shallow lacustrine model environments match the observed stratigraphy and facies of tectonostratigraphic unit 3. Model output is less satisfactory in explaining the middle and northern transects. In the middle transect, thick deposits of tectonostratigraphic unit 3 produce a major (>2 km) topographic high at the mountain front. Reduction of the frontal crustal load block (from 1.5 to 0.5 km) still produces significant subaerial topography in the proximal basin (Fig. 14), suggesting that either the stratigraphic thicknesses have been increased by thrust repetition, or that the model is unable to account for local structural or sediment discharge controls on isopachs. Conversely, the northern transect shows a deep (~1 km) proximal depression, even with a flexural rigidity of 10^{24} N m.

The mismatches between model output and observations of stratigraphic thicknesses and gross depositional environments do not follow a consistent trend, even within a single time slice. This indicates that the mismatches cannot be traced to a single cause. The marked along strike spatial variability in the Longmen Shan Foreland Basin stratigraphy, particularly during the late stages of basin evolution (tectonostratigraphic unit 3), cannot be explained by our simple one-dimensional model. It is possible throughout the modelling exercise that there are errors in the assumptions of linear elasticity, a continuous unbroken plate with constant flexural rigidity, and solely supracrustal loads. It is also possible that the heterogeneity of the South China lithosphere, specifically the presence of

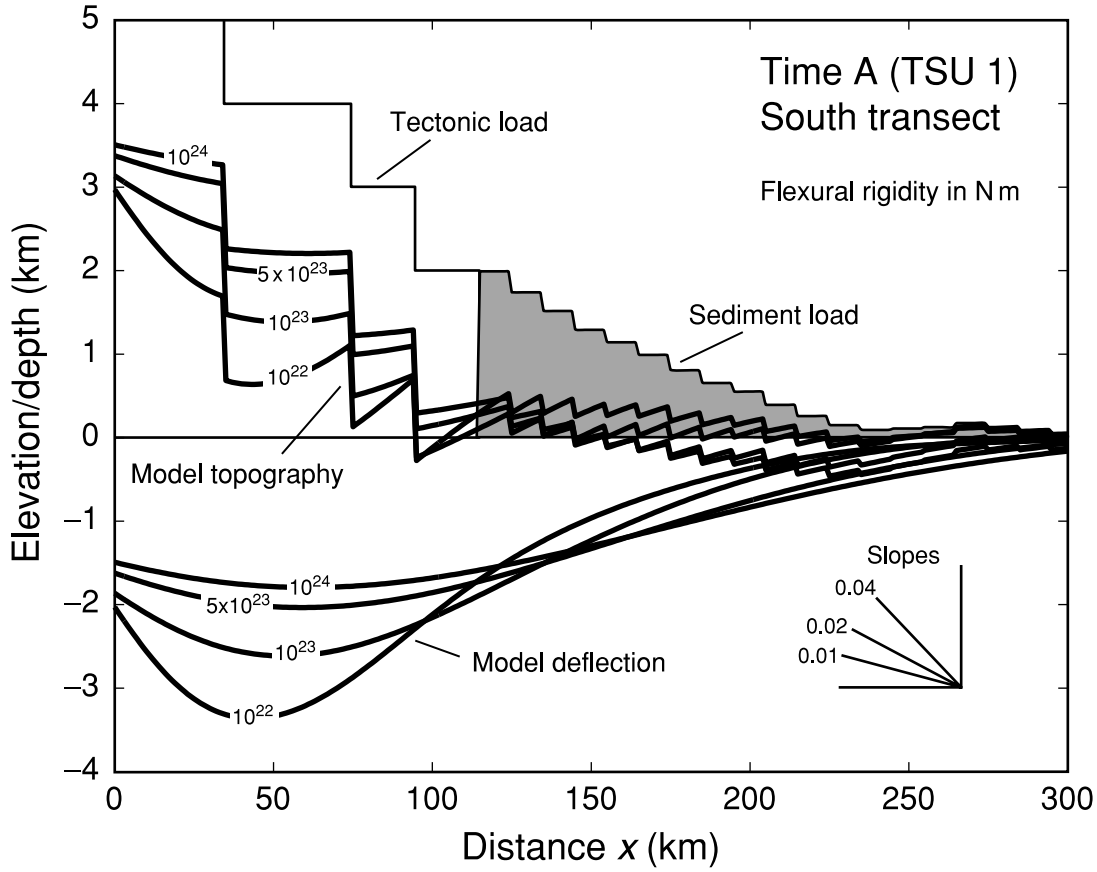

Fig. 11. Model topography/bathymetry and deflection for Time A (end of deposition of tectonostratigraphic unit 1, or TSU 1) along the southern transect, for a range of flexural rigidities of $10^{22}-10^{24}$ N m. Distance x increases to the southeast. The mountain front, and thus the front of the supracrustal tectonic load, is assumed to be at the palinspastically restored position of the Beichuan Fault, which is at $x = 120$ km. The thin black stairstep curve shows the supracrustal load imposed by the orogenic wedge. The shaded polygon shows the sediment load measured from the appropriate isopach maps (Figs 5–10). The heavy labelled lines show the calculated flexural deflection (smooth curve) and resulting topography (jagged curve) for different values of flexural rigidity (in N m). We estimate the most likely value of flexural rigidity by qualitatively comparing the topographic and bathymetric curves with (i) water depths inferred from gross depositional environments in the basin-fill and (ii) typical topographic profiles of mountain belts. In this case, the best fitting flexural rigidity is 5×10^{23} N m, since it predicts shallow marine depositional environments throughout the basin, deepening slightly to the west. We reject a lower flexural rigidity (e.g. 10^{22} N m), because that model predicts subaerial conditions across much of the foreland.

Table 2. Mean slopes calculated using 50–100 km-wide swaths across the flanks of major present-day mountain belts. The length of transect is the distance from the mountain front to the peak elevation.

Mountain front	Length of transect (km)	Slope	Degrees
Eastern Alps (Europe): S side	175	0.014	0.82
Eastern Alps (Europe): N side	122.5	0.015	0.85
Central Alps (Europe): S side	52	0.044	2.5
Central Alps (Europe): N side	88	0.023	1.3
Pyrenees: S side	110	0.019	1.1
Pyrenees: N side	38	0.049	2.8
Central Rocky Mountains	50	0.027	1.6
Himalayas: west	144	0.033	1.9
Himalayas: central	142	0.036	2.1
Himalayas: east	173	0.023	1.3

Table 3. Parameter values used in the analytical model.

Parameter values common to all model runs		
Young's modulus	E	70 GPa
Poisson's ratio	ν	0.25
Crustal density	ρ_c	2700 kg m^{-3}
Mantle density	ρ_m	3300 kg m^{-3}
Model run time A		
Infill density	ρ_i	2200 kg m^{-3}
Model run time B		
Infill density	ρ_i	2300 kg m^{-3}
Model run time C		
Infill density	ρ_i	2400 kg m^{-3}

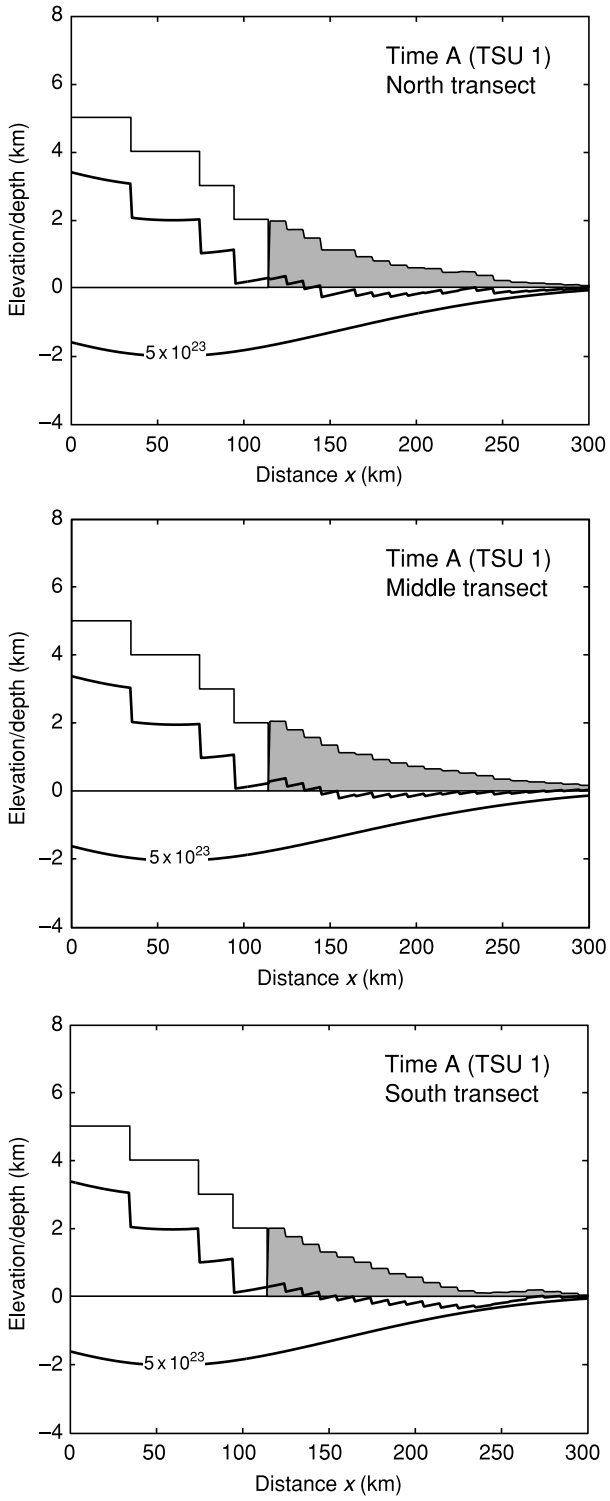

Fig. 12. Best-fitting model deflection and topography/bathymetry using the estimated loading configuration at Time A, equivalent to the end of deposition of tectonostratigraphic unit 1 (TSU 1), along the northern, middle and southern transects. Shallow-water environments across most of the foreland can be produced with a flexural rigidity of 5×10^{23} N m.

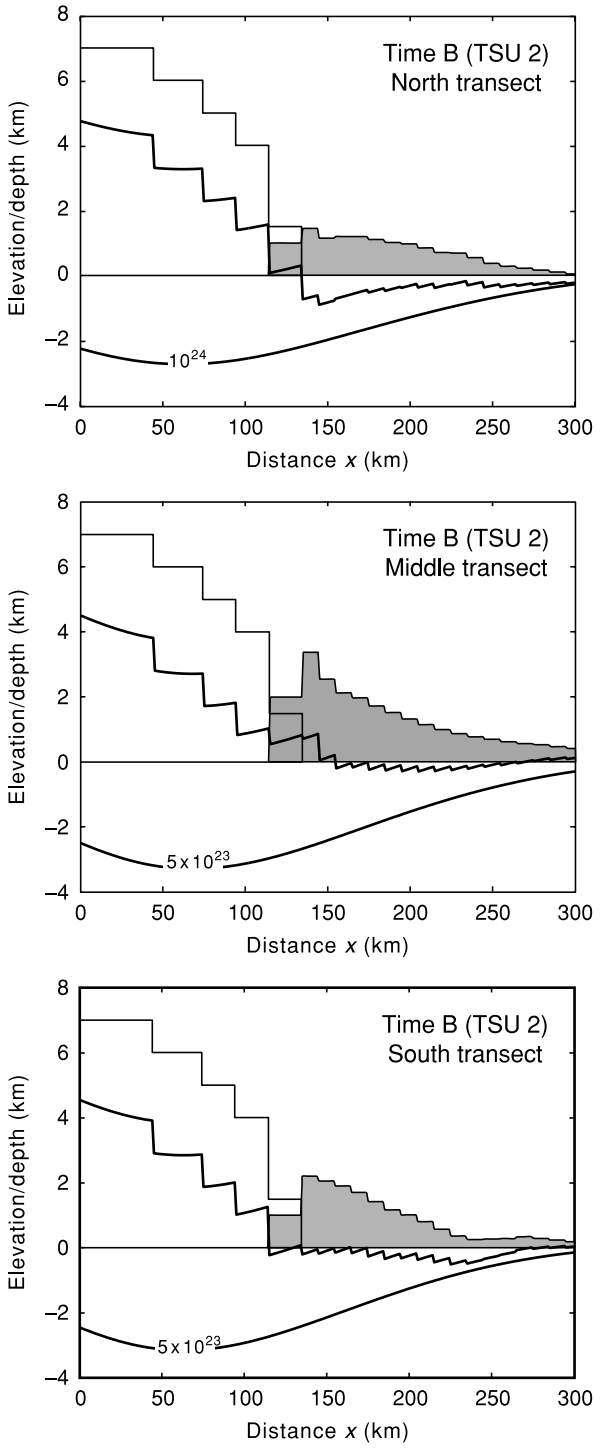

Fig. 13. Best-fitting model deflection and topography/bathymetry using the estimated loading configuration at Time B, equivalent to the end of deposition of tectonostratigraphic unit 2 (TSU 2), along the northern, middle and southern transects. Reasonable topographic profiles and lacustrine to subaerial depositional environments in the basin can be produced with flexural rigidities between 5×10^{23} and 5×10^{24} N m. Note that the supracrustal thrust loads have been increased relative to Time A and propagated a small distance (20 km, to $x = 140$ km) over the foreland.

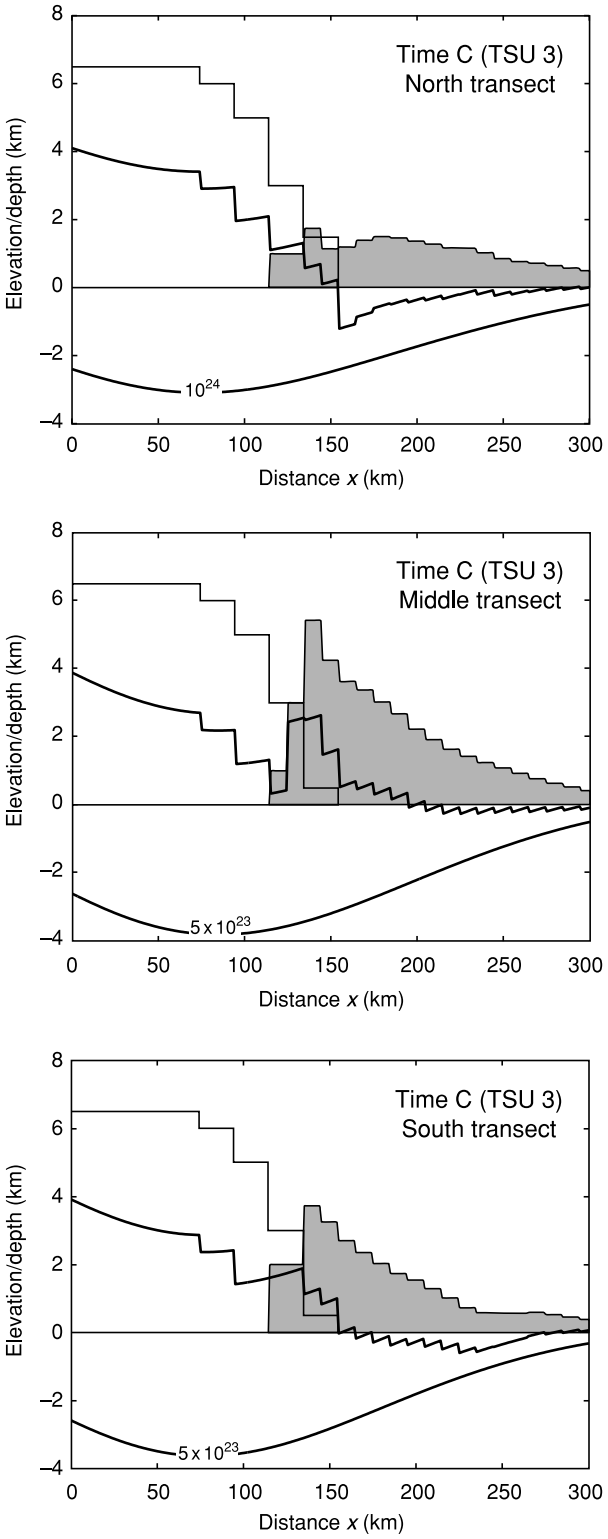

buried NE–SW orientated Permian graben beneath the foreland basin, may have influenced stratigraphic thicknesses. Nevertheless, there is in general a satisfactory first order explanation of foreland basin isopachs using a linear elastic continuous plate model with a constant Te of 45–50 km.

Stratigraphic data from the basin-fill, thrust timing inferred from the Longmen Shan Thrust Belt and insights derived from modelling are integrated in the chronostratigraphic diagram given in Fig. 15. The key features synthesised by this diagram are the widening stratigraphic gap along the basal megasequence boundary, the time-transgressive eastward migration of the foreland basin megasequence over the foreland of the South China Block, the switch from craton to orogenic sources though the development of the lowermost tectonostratigraphic unit (TSU 1), and the progradation of deltaic systems into firstly, open ocean, and subsequently, well-developed lake systems. The evolution of the Longmen Shan Foreland Basin was determined by the tectonic events taking place between the converging Qiangtang, North China–Kunlun–Qaidam, and South China Blocks, collectively resulting in the eastward propagation of an Indosinian orogenic wedge over the South China foreland (Fig. 16).

CONCLUSIONS

The Upper Triassic stratigraphy in the western Sichuan Basin comprises a foreland basin megasequence caused primarily by tectonic loading in the Longmen Shan and Songpan-Ganzi regions during the Indosinian Orogeny. The Indosinian Orogeny rapidly closed a deep, turbiditic trough in the Songpan-Ganzi zone and tectonically loaded the margin of the shallow-water carbonate-dominated South China Block, creating a flexural foredeep with a predominantly siliciclastic basin-fill in western Sichuan (Figs 15 and 16).

The sedimentary fill of the Longmen Shan Foreland Basin can be subdivided into three units. The first tectonostratigraphic unit overlies a flexural forebulge unconformity and initially records the establishment and drowning of a carbonate ramp and sponge build-up along the forebulge margin of the marine basin. Further generation of accommodation caused by basinward migration of the load system resulted in a deepening of depositional environments, followed by progradation of fluvial-dominated deltas sourced from the orogen. Loss of the connection of the basin with the open ocean caused delta systems to prograde into a basinal lake system by the close

Fig. 14. Best-fitting model deflection and topography/bathymetry using the estimated loading configuration at Time C, equivalent to the end of deposition of tectonostratigraphic unit 3 (TSU 3), along the northern, middle and southern transects. A reasonable topographic profile and subaerial to lacustrine depositional environments in the basin can be produced with flexural rigidities of $5 \times 10^{23} - 5 \times 10^{24}$ N m along the southern transect. In the middle transect, the best-fitting flexural rigidity produces an unacceptable positive feature reaching over 2 km in elevation in the proximal basin. In the northern transect, unacceptably large lake water depths (< 1 km) are produced in proximal basin positions. These mismatches highlight the inadequacy of the one-dimensional model to deal with large along-strike spatial variations in sediment discharges and subsidence rates in some basin compartments. Note that the supracrustal thrust loads have been propagated a small distance (20 km, to $x = 160$ km) over the foreland relative to Time B.

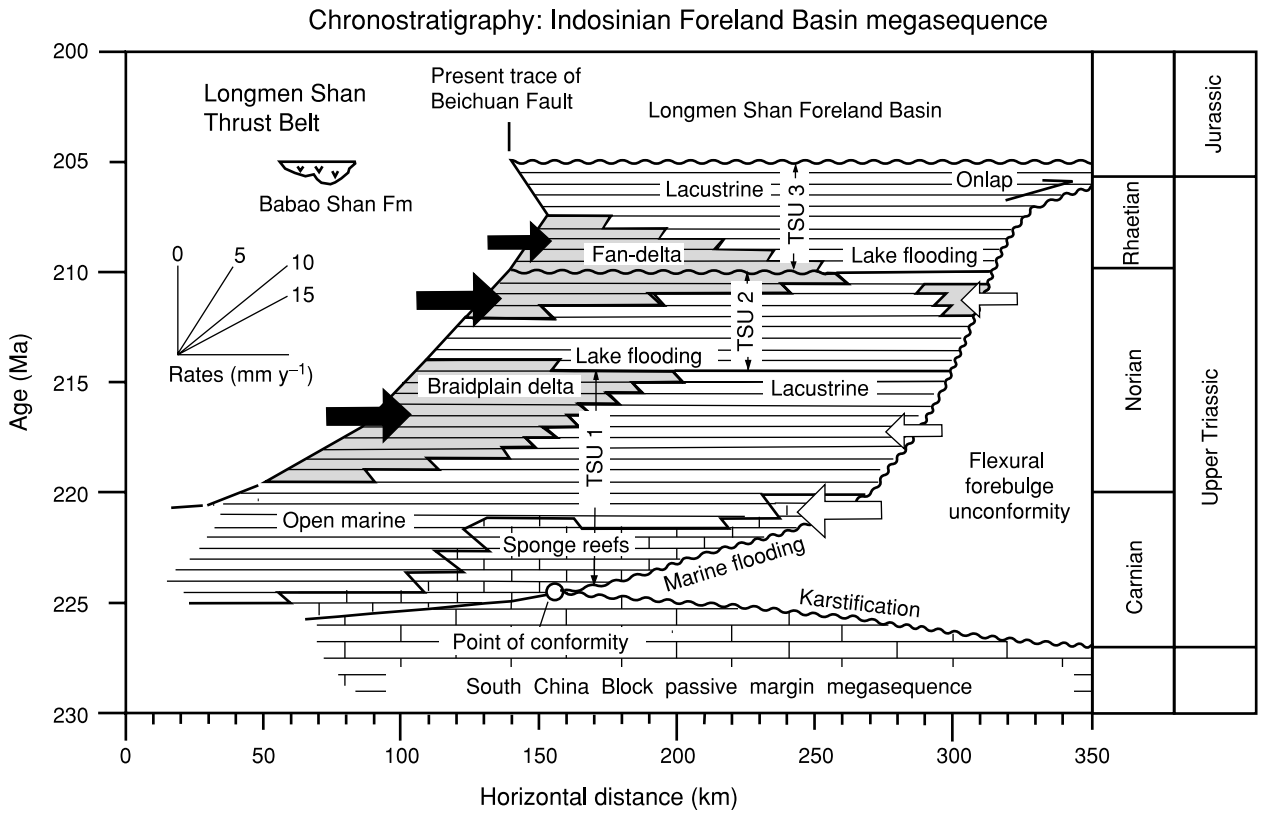

Fig. 15. Chronostratigraphic chart for the Foreland Basin, based on the available stratigraphic data and insights derived from modelling. Within the foreland basin megasequence, there is a change from craton-derived sediment supply (unfilled arrows) during early TSU 1, to dual supply in mid-TSU 1, followed by dominance by orogenic sources (filled arrows) thereafter. The basal boundary of the foreland basin megasequence is a flexural forebulge unconformity. Tectonostratigraphic units are bounded by marine (TSU 1) or lake (TSU 2 and TSU 3) flooding events. The transition from underfilled to filled status takes place late in TSU 1, after which the connection with the ocean is closed.

of this tectonostratigraphic unit. Tectonostratigraphic unit 2 was initiated by a major lake flooding event, and comprises a thick upward-coarsening cycle due to delta progradation. The third tectonostratigraphic unit is recognised by an erosional base that truncates tectonostratigraphic unit 2 and is composed of an upward-fining cycle from coarse proximal fan-deltas to open lacustrine shales, indicating retrogradation of the basin margin.

We interpret the stratigraphic architecture as driven by the initially rapid (c. 15 mm yr^{-1}) migration of an orogenic wedge over a relatively rigid foreland plate ($D = 5 \times 10^{23} - 5 \times 10^{24}$ Nm, Te ~50 km) during the deposition of tectonostratigraphic unit 1. Slowing of the thrust advance rate (c. 5 mm yr^{-1}) and thickening and steepening of the orogenic wedge caused high sediment fluxes from the orogen during the deposition of tectonostratigraphic units 2 and 3. An analytical model of supracrustal loading of a continuous linear elastic plate achieves a promising simulation of the general form of three transverse profiles in the basin, with the exception of the middle and northern transects at the end of deposition of tectonostratigraphic unit 3. Possible complexities may include the presence of additional subcrustal or in-plane loads, supracrustal loads not represented by the Longmen Shan orogen, a broken rather than continuous plate under the orogen, and plate inelasticity as well as the influence of underlying Permian extensional fault structures, none of which have been incorporated in the analytical model. There is no indication of a secular change in flexural rigidity of the South China Block during the c. 20 Myr time span of the Indosinian foreland basin megasequence.

ACKNOWLEDGEMENTS

This study was initiated during an academic visit to Trinity College Dublin by Li Yong of the Chengdu University of Technology in Chengdu, China and was completed at the Swiss Federal Institute of Technology (ETH Zürich). This research was supported by grants from the National Science Foundation of China (Grant 49803013), Foundation Grants for Young Geologists of GMR (Qn979816), and the China Scholarship Council. ALD acknowledges support from the Enterprise Ireland International Collaboration Programme (Grant IC/2000/064). Joana Gafeira compiled the mountain front data in Table 2. We thank Peter DeCelles, B.C. Burchfiel, Stephan Graham, and Eric Kirby for constructive and helpful reviews. We are especially grateful for the continual support and encouragement of Zeng Yunfu, He Zhenghua, Wang Chengshan and Chen Hongde.

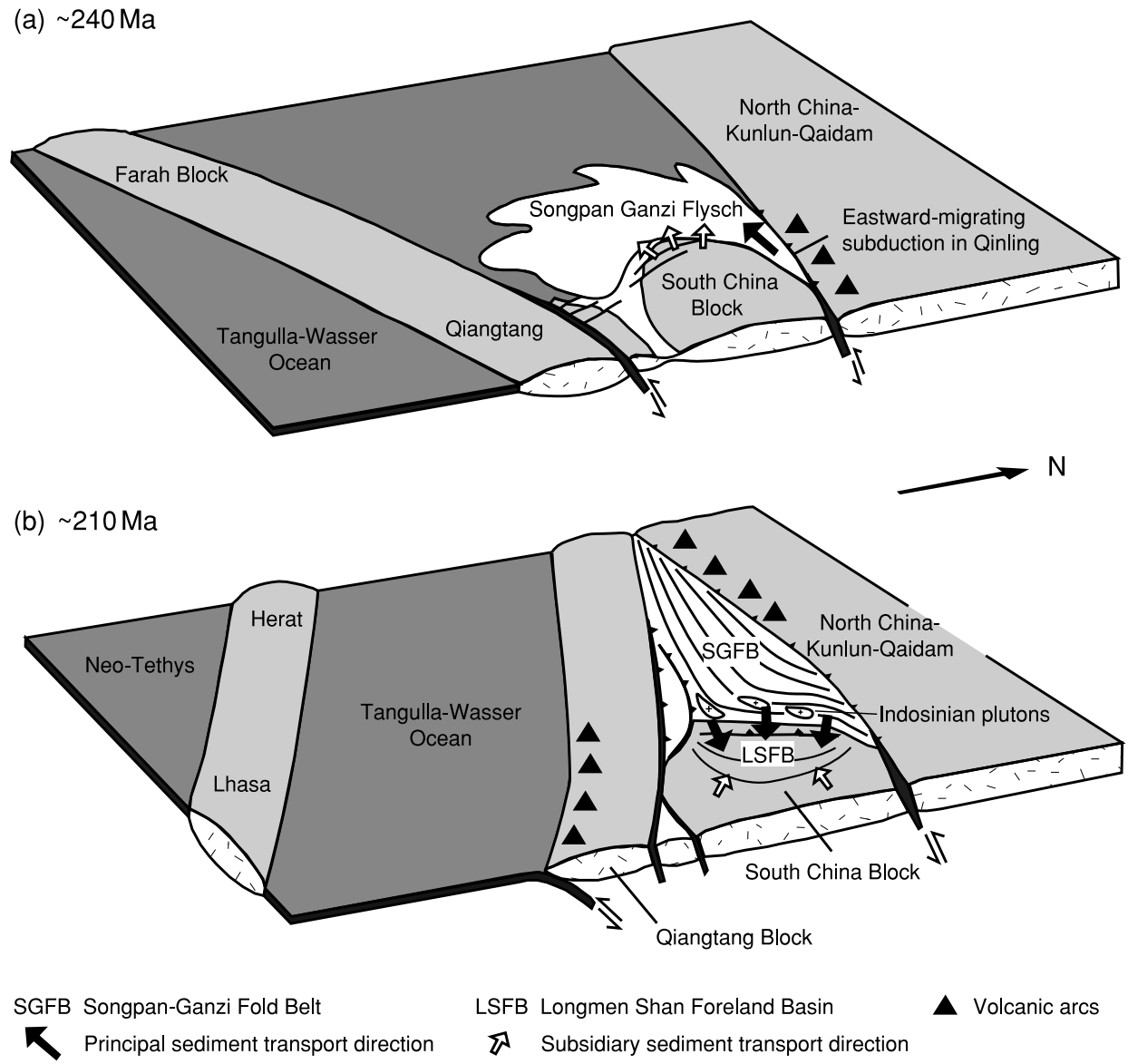

Fig. 16. Cartoons showing geological evolution from South China Block passive margin flanking a deep remnant ocean basin accumulating sediments of the Songpan-Ganzi Complex in (a), to oceanic closure, telescoping of the Songpan-Ganzi Complex and South China margin and formation of the Longmen Shan Foreland Basin as a flexural foredeep in (G). Modified from Harrowfield (2001).

REFERENCES

Allen, P.A. & Allen, J.R. (1990) *Basin Analysis: principles and Applications*, p. 461. Blackwell Science, Oxford.

Allen, P.A., Burgess, P.M., Galewsky, J. & Sinclair, H.D. (2001) Flexural-eustatic numerical model for drowning of the Eocene perialpine ramp and implications for Alpine geodynamics. *Bull. Geol. Soc. Am.*, **113,** 1052–1066.

Allen, P.A., Crampton, S.L. & Sinclair, H.D. (1991) The inception and early evolution of the North Alpine foreland basin. *Basin Res.*, **4,** 143–163.

Allen, P.A., Homewood, P. & Williams (1986) Foreland basins: an introduction. In: *Foreland Basins* (Ed. by P.A. Allen & P. Homewood). *Spec. Publ. Int. Assoc. Sediment.*, **8,** 3–12.

Athy, L.F. (1930) Density, porosity and compaction of sedimentary rocks. *Bull. Am. Assoc. Petrol. Geol.*, **14,** 1–24.

Beaumont, C. (1981) Foreland basins. *Geophys. J. Royal Astronom. Soc.*, **65,** 291–329.

Beaumont, C., Fullsack, P. & Hamilton, J. (1991) Erosional control of active compressional orogens. In: *Thrust Tectonics* (Ed. by K. McClay), pp. 1–18. Chapman & Hall, London.

Burchfiel, B.C., Chen, Z., Liu, Y. & Royden, L.H. (1995) Tectonics of the Longmen Shan and adjacent regions, Central China. *Int. Geol. Rev.*, **37,** 661–735.

Cardozo, N. & Jordan, T. (2001) Causes of spatially variable tectonic subsidence in the Miocene Bermejo foreland basin, Argentina. *Basin Res.*, **13,** 335–357.

Chen, S.F. & Wilson, C.J.L. (1996) Emplacement of the Longmen Shan Thrust-Nappe Belt along the eastern margin of the Tibetan Plateau. *J. Struct. Geol.*, **18,** 413–430.

Chen, S.F., Wilson, C.J.L., Luo, Z.L. & Deng, Q.D. (1994) The evolution of the Longmen Shan foreland basin. *J. Southeast Asian Earth Sci.*, **10,** 159–168.

Chen, S.F., Wilson, C.J.L. & Worley, B.A. (1995) Tectonic transition from the Songpan-Garze fold belt to the Sichuan basin, southwestern China. *Basin Res.*, **7,** 235–253.

Coakley, B.J. & Watts, A.B. (1991) Tectonic controls on the development of unconformities: the North Slope Alaska. *Tectonics*, **10,** 101–130.

Covey, M. (1986) The evolution of foreland basins to steady state: evidence from the western Taiwan foreland basins. In: *Foreland Basins*, Vol. 8 (Ed. by P.A. Allen & P. Homewood). *Spec. Publ. Int. Assoc. Sediment.* Blackwell Science, Oxford.

Crampton, S.L. & Allen, P.A. (1995) Recognition of flexural forebulge unconformities associated with early stage foreland basin development: Example from the North Alpine foreland basin. *Bull. Am. Assoc. Petrol. Geol.*, **79,** 1495–1514.

Decelles, P.G. & Giles, K.A. (1996) Foreland basin systems. *Basin Res.*, **8,** 105–125.

Decelles, P.G. & Mitra, G. (1995) History of the Sevier orogenic wedge in terms of critical taper models, northeast Utah and southeast Wyoming. *Bull. Geol. Soc. Am.*, **107,** 454–462.

Deng, K.L., He, L., Qin, D.Y. & He, Z.G. (1982) The earlier Late Triassic sequence and its sedimentary environment in western Sichuan basin. *Oil Gas Geol.*, **3,** 200–210.

Deng, K.L. & Li, G.J. (1987) A preliminary discussion of turbidity deposits in Aba region, Sichuan. In: *Collected Works on Lithofacies and Palaeogeography*, Vol. 4, pp. 129–138. Geological Publishing House, Beijing.

Dorobek, S.L. (1995) Synorogenic carbonate platforms and reefs in foreland basins: controls on stratigraphic evolution and platform/reef morphology. In: *Stratigraphic Evolution of Foreland Basins* (Ed. by S.L. Dorobek & G.M. Ross), *Spec. Publ. Soc. Sedimen. Geol. (SEPM)*, **52,** 127–147.

Flemings, P.B. & Jordan, T.E. (1989) A synthetic stratigraphic model of foreland basin development. *J. Geophys. Res.*, **94,** B3851–B3866.

Flemings, P.B. & Jordan, T.E. (1990) Stratigraphic modelling of foreland basins: interpreting thrust deformation and lithospheric rheology. *Geology*, **18,** 430–435.

Galewsky, J. (1998) The dynamics of foreland basin carbonate platforms: tectonic and eustatic controls. *Basin Res.*, **10,** 409–416.

Gradstein, F.M., Agtenberg, F.P., Ogg, J.G., Hardenbol, J., van Veen, P., Thierry, J. & Huang, Z. (1995) A Triassic, Jurassic and Cretaceous time scale. In: *Geochronology, Time Scales and Global Stratigraphic Correlation*, Vol. 54 (Ed. by W.A. Berggren, D.V. Kent, M.-P. Aubry & J. Hardenbol), pp. 95–126. Society of Economic Paleontologists and Petrologists Special Publication, Tulsa.

Guo, Z.W., Deng, K.L. & Han, Y.H. *et al.* (1996) *The Formation and Development of Sichuan Basin*, p. 200. Geological Publishing House, Beijing.

Harrowfield, M.J. (2001) *The Tectonic Evolution of the Songpan Garze Fold Belt, Southwest China*. Unpublished PhD Thesis, p. 271. University of Melbourne, Australia.

He, L. (1989) The classification and correlation of Upper Triassic seismic stratigraphy in Sichuan Basin. *Oil Gas Geol.*, **10,** 441–445.

Heller, P.L., Angevine, C.L., Winslow, N.S. & Paola, C. (1988) Two phase stratigraphic model of foreland basin sequences. *Geology*, **16,** 501–504.

Hetenyi, M. (1946) *Beams on Elastic Foundations*. The University of Michigan Press.

Homewood, P., Allen, P.A. & Williams, G.D. (1986) Dynamics of the Molasse basin in western Switzerland. In: *Foreland Basins*, Vol. 8 (Ed. by P.A. Allen & P. Homewood), 199–217, *Spec. Publ. Int. Assoc. Sediment.*, Blackwell Science, Oxford.

Hong, Z. (1991) *Regional Geology of Sichuan Province*, pp. 690–730. Geological Publishing House, Beijing.

Hu, S.H., Luo, D.X. & Li, K.Y. (1983) Triassic sedimentary facies in east Xizang-west Sichuan and their tectonic significance. *Contrib. Geol. Qinghai-Xizang (Tibet) Plateau*, **13,** 107–128.

Hu, Q. & Yan, Y.L. (1987) Research in west of Sichuan basin by seismic stratigraphy. *Geophys. Prospect. Petrol.*, **26,** 16–29.

Huang, J.Q. & Chen, B.W. (1987) *The Evolution of the Tethys in China and Adjacent Regions*. Geological Publishing House, Beijing.

Hubbard, R.J., Pape, J. & Roberts, D.G. (1985) Depositional sequence mapping as a technique to establish tectonic and stratigraphic framework and evaluate hydrocarbon potential on a passive continental margin. In: *Seismic Stratigraphy II: An Integrated Approach* (Ed. by O.R. Berg & D. Woolverton). *Am. Assoc. Petrol. Geol. Memoir.*, **39,** 79–91.

Ingersoll, R.V., Graham, S.A. & Dickinson, W.R. (1995) Remnant ocean basins. In: *Tectonics of Sedimentary Basins* (Ed. by C. Busby & R.V. Ingersoll), pp. 1–51. Blackwell Science, Oxford.

Jacobi, R.D. (1981) Peripheral bulge – a causal mechanism for the lower/middle Ordovician unconformity along the western margin of the northern Appalachians. *Earth Planet. Sci. Lett.*, **56,** 245–251.

Johnson. D.D. & Beaumont, C. (1995) Preliminary results from a planform kinematic model of orogen evolution, surface processes and the development of clastic foreland basin stratigraphy. In: *Stratigraphic Evolution of Foreland Basins*, Vol. 52 (Ed. by S.L. Dorobek & G.M. Ross), pp. 3–24, *Spec. Publ. Soc. Sediment. Geol. (SEPM)*, Tulsa, Oklahoma.

Jordan, T.E. (1981) Thrust loads and foreland basin evolution, Cretaceous, western United States. *Bull. Am. Assoc. Petrol. Geol.*, **65,** 2506–2520.

Kirby, E., Whipple, K.X., Burchfiel, B.C., Tang, W., Berger, G., Sun, Z. & Chen, Z. (2000) Neotectonics of the Min Shan, China: implications for mechanisms driving Quaternary deformation along the eastern margin of the Tibetan Plateau. *Geol. Soc. Am. Bull.*, **112,** 375–393.

Korsch, R.J., Mai, H., Sun, Z. & Gorter, J.D. (1997) Evolution and subsidence history of the Sichuan basin, southwest China. In: *Proceedings of the 30th International Geological Congress, China*, Vol. 8 (Ed. by Liu Baojun, *et al.*), pp. 208–221.

Kühni, A. & Pfiffner, O.A. (2001) Drainage patterns and tectonic forcing: a model for the Swiss Alps. *Basin Res.*, **13,** 169–198.

Li, Y., Zeng, Y. & Yi, H. (1995) *Sedimentary and tectonic evolution of the Longmen Shan Foreland Basin, Western Sichuan, China (in Chinese)*, pp. 1–92. Press of Chengdu University of Science and Technology, Chengdu.

Lin, M.B., Gou, Z.H., Wang, G.Z., Deng, J.H., Li, Y., Wang, D.Y. & Hu, X.W. (1996) *Geology in Middle Section of Longmen Mountains*, pp. 1–221. Press of Chengdu University of Science and Technology, Chengdu.

Liu, X., Fu, D., Yao, P., Liu, G. & Wang, N. (1992) The Stratigraphy, *Paleobiogeography and Sedimentary-Tectonic Development of Qinghai-Xizang (Tibet) Plateau in Light of Terrane Analysis (English Abstract)*, pp. 151–169. Geological Publishing House, Beijing.

Liu, X. & Zhou, P. (1982) Late Triassic. In: *Continental Mesozoic Stratigraphy and Paleontology in Sichuan Basin of China*. pp. 1–236. People's Publishing House of Sichuan, Chengdu.

Long, X. (1991) Several questions of geochronic evolution in the mid-northern segment of the Longmen Shan Mountains. *J. Chengdu College Geol.*, **18,** 8–16.

Luo, Z., Jin, Y. & Zhao, X. (1990) The Emei taphrogenesis of the Upper Yangtze Platform in south China. *Geol. Magazine*, **127,** 393–405.

Luo, Z. & Long, X. (1992) The uplifting of the Longmen Shan orogenic zone and the subsidence of the West Sichuan foreland basin. *Acta. Geol. Sichuan*, **12,** 1–17.

Martin-Martin, M., Rey, J., Alcala-Garcia, F.J., Tosquella, J., Deramond, J., Lara-Corona, E., Duranthon, F. & Antoine, P.-O. (2001) Tectonic controls on the deposits of a foreland basin: an example from the Eocene Corbières-Minérvois basin, France. *Basin Res.*, **13,** 419–433.

Miall, A.D. (1978) Tectonic setting and syndepositional deformation of molasse and other nonmarine-paralic sedimentary basins. *Can. J. Earth Sci.*, **15,** 1613–1632.

Quinlan, G.M. & Beaumont, C. (1984) Appalachian thrusting, lithospheric flexure, and the Palaeozoic stratigraphy of the eastern interior of North America. *Can. J. Earth Sci.*, **21,** 973–996.

Rao, R.B. & Xu, J.F. (1987) *The Triassic System of the Qinghai-Xizang Plateau*, pp. 201–239. Geological Publishing House, Beijing.

Regional Geological Map and Report of Longmen Shan (1995) *Bureau of Geology and Mineral Resources of Sichuan Province*, People's Publishing House of Sichuan, Chengdu.

Regional Geology of Sichuan Province (1991) *People's Republic of China Ministry of Geology and Mineral Resources, Geological Memoirs.* Series 1, no. 23. Geological Publishing House, Beijing.

Saylor, B.Z., Grotzinger, J.P. & Germs, G.J.B. (1995) Sequence stratigraphy and sedimentology of the Neoproterozoic Kuibis and Schwarzrand Subgroups (Nama Group), southwestern Namibia. *Precambrian Res.*, **73,** 153–171.

Schlunegger, F. (1999) Controls of surface erosion on the evolution of the Alps: constraints from the stratigraphies of the adjacent foreland basins. *Int. J. Earth Sci.*, **88,** 285–304.

Schlunegger, F., Melzer, J. & Tucker, G.E. (2001) Climate, exposed source-rock lithologies, crustal uplift and surface erosion: a theoretical analysis calibrated with data from the Alps/North Alpine foreland basin system. *Int. J. Earth Sci. (Geologisches Rundschau)*, **90,** 484–499.

Schlunegger, F. & Willett, S.D. (1999) Spatial and temporal variations in exhumation of the central Swiss Alps and implications for exhumation mechanisms. *Geol. Soc. London Spec. Publ.*, **154,** 157–179.

Sclater, J.G. & Christie, P.A.F. (1980) Continental stretching: an explanation of the post-Mid–Cretaceous subsidence of the central North Sea basin. *J. Geophys. Res.*, **85,** 3711–3739.

Sengör, A.M.C. (1985) The Cimmeride orogenic system and the tectonics of Eurasia. *Geol. Soc. Am. Spec. Paper*, **195**, p. 82.

Shu, W., Yan, H., Zhou, Z. & He, L. (1988) *Sedimentary Environment of Upper Triassic Coal Measures in Sichuan Basin. Spec. Publ. Oil and Gas*, Vol. 1, pp. 196–208. Geological Publishing House, Beijing.

Sinclair, H.D. (1997) Tectonostratigraphic model of underfilled peripheral foreland basins: an Alpine perspective. *Bull. Geol. Soc. Am.*, **109,** 323–346.

Sinclair, H.D. & Allen, P.A. (1992) Vertical versus horizontal motions in the Alpine orogenic wedge: stratigraphic response in the foreland basin. *Basin Res.*, **4,** 215–232.

Sinclair, H.D., Coakley, B.C., Allen, P.A. & Watts, A.B. (1991) Simulation of foreland basin stratigraphy using a diffusion model of mountain belt uplift and erosion: an example from the Central Alps, Switzerland. *Tectonics*, **10,** 599–620.

Stewart, J. & Watts, A.B. (1997) Gravity anomalies and spatial variations of flexural rigidity at mountain ranges. *J. Geophys. Res.*, **102,** 5327–5352.

Stockmal, G.S. & Beaumont, C. (1987) Geodynamic models of convergent margin tectonics: the southern Canadian Cordillera and the Swiss Alps. *Can. Soc. Petrol. Geol. Memoir.*, **12,** 393–411.

Stockmal, G.S., Beaumont, C. & Boutilier, R. (1986) Geodynamic models of convergent tectonics: the transition from rifted margin to overthrust belt and consequences for foreland basin development. *Bull. Am. Ass. Petrol. Geol.*, **70,** 181–190.

Turcotte, D.L. & Schubert, G. (1982) *Geodynamics: applications of Continuum Mechanics to Geological Problems*. p. 450. Wiley, New York.

Wang, J.Q. (1990) Anxian tectonic movement (in Chinese). *Oil Gas Geol.*, **11,** 223–234.

Wang, J., Bao, C., Luo, Z. & Guo, Z. (1989) Formation and development of the Sichuan Basin. In: *Chinese Sedimentary Basins* (Ed. by X. Zhu), pp. 147–163. Elsevier.

Watson, M.P., Hayward, A.B., Parkinson, D.N. & Zhang, Z.M. (1987) Plate tectonic history, basin development and petroleum source rock deposition onshore China. *Mar. Petrol. Geol.*, **4,** 205–225.

Watts, A.B. (1992) The effective elastic thickness of the lithosphere and the evolution of foreland basins. *Basin Res.*, **4,** 169–178.

Whiting, B.M. & Thomas, W.A. (1994) Three-dimensional controls on subsidence of a foreland basin associated with a thrust belt recess: Black Warrior basin, Alabama and Mississippi. *Geology*, **22,** 727–730.

Xu, Z.Q., Hou, L.W., Wang, D.K. & Wang, Z.X. (1992) *Orogenic Processes of the Songpan-Garze Orogenic Belt of China*. Geological Publishing House, Beijing.

Yang, X. (1982) Late Triassic plant fossils in Sichuan Basin. In: *Continental Mesozoic Stratigraphy and Paleontology in Sichuan Basin of China*, pp. 462–490. People's Publishing House of Sichuan, Chengdu.

Yin, A. & Nie, S. (1996) A Phanerozoic palinspastic reconstruction of China and its neighboring regions. In: *The Tectonic Evolution of Asia* (Ed. by A. Yin & T.M. Harrison). pp. 442–485. Cambridge University Press, Cambridge.

Zhang, Q. (1981) The sedimentary features of the flysch formation of the Xikaang group in the Indosinian Songpan-Garze geosyncline and its geotectonic setting. *Geol. Rev.*, **27,** 405–412.

Zhou, D. & Graham, S.A. (1996) The Songpan-Ganzi complex of the West Qinling Shan as a Triassic remnant ocean basin. In: *The Tectonic Evolution of Asia* (Ed. by A. Yin & T.M. Harrison). pp. 281–299. Cambridge University Press, Cambridge.

Zou, D., Chen, L., Rao, R. & Chen, Y. (1984) On the Triassic turbidites in the southern Baryanhar Mountain region. *Contributions Geol. Qinghai-Xizang (Tibet) Plateau*, **15,** 27–39.

Manuscript received 20 December 2001; Manuscript revised 15 October 2002; Manuscript accepted 08 November 2002

